OPTIMIZED SCHWARZ METHODS FOR BIHARMONIC EQUATIONS*

MARTIN J. GANDER† AND YONGXIANG LIU‡

Abstract. We are interested in Schwarz domain decomposition methods for the biharmonic equation. In contrast to the Laplace case, this is a fourth-order partial differential equation and thus requires two boundary conditions, and not just one, which implies also that Schwarz methods will need to use two transmission conditions between subdomains, and not just one. As we showed in [11], there are many choices of Dirichlet and Neumann conditions for biharmonic problems, which lead to various Dirichlet-Neumann domain decomposition algorithms with different convergence rates. A Robin type boundary condition consists in general of a linear combination of Dirichlet and Neumann conditions. We choose here different sets of Dirichlet and Neumann conditions, and thus we obtain several different optimized Schwarz methods. We prove that by optimizing the Robin matrices (not just scalars), the convergence rates become the same as for optimized Schwarz methods for the Laplace problem, for two of the variants which is better than what is usually achieved for the biharmonic equation. We present numerical experiments, including also situations not covered by our analysis, and as application a simulation of the Golden Gate Bridge.

Key words. Biharmonic equations, Optimized Schwarz methods, Transmission conditions.

AMS subject classifications. 65N22, 65N55, 65F08, 65F10.

1. Introduction.

Our goal is to formulate and analyze Schwarz methods for solving biharmonic problems of the form

$$\Delta^2 u = f \quad \text{in } \Omega, \quad u = 0 \quad \text{and} \quad \partial_n u = 0 \quad \text{on } \partial\Omega. \tag{1.1}$$

Here the domain $\Omega \subset \mathbb{R}^2$, f is a right hand side function, and ∂_n is the normal derivative on the boundary $\partial\Omega$.

The biharmonic operator contains up to fourth-order derivatives, and one thus needs two boundary conditions, in contrast to the classical Laplace operator, where one only needs one. There are two different mathematical interpretations for the biharmonic problem (1.1): one is modeling thin plate bending problems and vibrations, and the other is related to the Stokes problem arising from solving incompressible viscous fluid problems in 2D, see, e.g., [11].

The homogeneous boundary conditions we chose to impose in (1.1) both on the traces and the normal derivatives are often considered to be the Dirichlet condition,

$$\mathcal{D}_1(u) := \begin{bmatrix} u \\ \partial_n u \end{bmatrix}, \tag{1.2}$$

which is widely used for designing corresponding domain decomposition methods. For example, a direct application is the classical Schwarz domain decomposition algorithm. Zhang analyzed in [18] for conforming C^1 finite elements the corresponding two-level additive Schwarz method, and showed that with subdomain size H and overlap $\delta = O(H)$ the condition number is independent of H and the mesh size h. For

*Submitted. This work is an extension of our conference proceeding [10] and combines proofs of results announced therein.

Funding: Supported by the Chinese National Science Foundation (No. 11701536).

†University of Geneva, Section of Mathematics, Rue du Conseil-Général 9, CP 64 CH-1211 Genève 4, (Martin.Gander@unige.ch).

‡Pengcheng Laboratory, Shenzhen 518055, China, (Corresponding author: liuyx@pcl.ac.cn).

nonconforming finite elements, Brenner proved in [1] for the additive Schwarz preconditioner a condition number bound $C(1+\frac{H}{\delta})^4$ for large overlap and $C(1+\frac{H}{\delta})^3$ for small overlap. For Morley finite element discretizations, an additive average Schwarz method was proposed by Feng and Rahman in [6], with a condition number estimate of $O(1+\frac{H}{h})^3$. Feng and Karakashian introduced in [5] a non-overlapping Schwarz preconditioner in the context of discontinuous Galerkin methods and derived a condition number bound of $O(1+\frac{H}{h})^3$. By using the $\mathcal{D}_1$ condition in the alternating Schwarz method, the corresponding convergence factor is $1-O(\delta^3)$, also with the power 3 as in the condition number estimates, for details see Section 2.

There are two possibilities to choose Neumann boundary conditions corresponding to the classical Dirichlet condition (1.2). If the problem is understood as coming from the Stokes case, the corresponding Neumann condition would be

$$\mathcal{N}_1(u) := \begin{bmatrix} \Delta u \\ -\partial_n \Delta u \end{bmatrix}. \tag{1.3}$$

If it is understood as the thin plate bending case, then it would be

$$\mathcal{N}_2(u) := \begin{bmatrix} \Delta u - (1-\sigma)\partial_{\tau\tau} u \\ -\partial_n \Delta u - (1-\sigma)\partial_\tau(\partial_{n\tau} u) \end{bmatrix}, \tag{1.4}$$

where σ is a material constant called the Poisson's ratio which lies in $[0,\frac{1}{2}]$, and τ is the tangential derivative along the boundary with the normal direction n and tangential direction τ forming a right-handed coordinate system (n,τ). However, one can mathematically also enlarge the range of σ to $\sigma \in (-1,1)$, and the problem with Neumann condition (1.4) remains well-posed, while condition (1.3) might not lead to a well-posed problem [11]. For the thin plate problem, condition (1.4) corresponds to a freely supported boundary condition and is always well-posed up to a linear function. However, Robin boundary conditions which combine (1.2) with (1.3) or (1.4) can both lead to well-posed problems, as we will show later.

There are many domain decomposition methods for solving the thin plate problem that use the Neumann condition (1.4): a Neumann-Neumann-type preconditioner was presented by Tallec, Mandel, and Vidrascu in [13], with a condition number estimate of $O(1+\log\frac{H}{h})^2$. A substructuring method was presented by Dohrmann in [2] including constraints on the substructure boundary, and Mandel and Dohrmann proved in [14] the associated condition number estimate to be of $O(1+\log\frac{H}{h})^2$. FETI methods for the biharmonic problem were proposed and studied by Farhat and Mandel in [4], see also Mandel, Tezaur and Farhat [15], where continuity of transverse displacements is imposed at cross points, and the condition number was estimated to be $O(1+\log\frac{H}{h})^3$. A Dirichlet-Neumann method for a biharmonic problem including lower-order terms was introduced by Gervasio in [12]. To define the method, Gervasio first transformed the problem into an equivalent system involving two Poisson equations, and then used $\mathcal{D}_1$ as Dirichlet condition, and a condition similar to $\mathcal{N}_2$ as Neumann condition. This led to a contraction estimate, but without any optimization. Nourtier-Mazauric and Blayo introduced for the time-dependent biharmonic problem an optimized Schwarz waveform relaxation method based on combining (1.2) with (1.3), and illustrated its performance by numerical experiments.

Instead of the classical clamped Dirichlet conditions (1.2) (and associated Neumann condition (1.3)), one could also consider

$$\mathcal{D}_3(u) := \begin{bmatrix} u \\ \Delta u \end{bmatrix}, \quad \mathcal{N}_3(u) := \begin{bmatrix} \partial_n u \\ -\partial_n \Delta u \end{bmatrix}, \tag{1.5}$$

see for example [3]. Similarly, in the thin plate case, instead of (1.2) and (1.4), another choice for the Dirichlet and Neumann conditions would be

$$\mathcal{D}_4(u) := \begin{bmatrix} u \\ \Delta u - (1-\sigma)\partial_{\tau\tau} u \end{bmatrix}, \quad \mathcal{N}_4(u) := \begin{bmatrix} \partial_n u \\ -\partial_n \Delta u - (1-\sigma)\partial_\tau(\partial_{n\tau} u) \end{bmatrix}. \tag{1.6}$$

For flat boundaries, (1.5) and (1.6) are basically equivalent, since imposing u also means imposing $\partial_{\tau\tau}$. For curved boundaries however, these conditions are different, as one can see by direct calculations, and hence they would also be different as transmission conditions in domain decomposition methods. By using $\mathcal{D}_3$ or $\mathcal{D}_4$ in the alternating Schwarz method, the corresponding convergence factor is $1 - O(\delta)$, which is of order 1 and better than the $\mathcal{D}_1$ condition case, see Section 2.

We know that for the Poisson problem,

$$-\Delta u = f \quad \text{in } \Omega, \quad u = 0 \quad \text{on } \partial\Omega,$$

the Dirichlet condition is $\mathcal{D}_{Poisson}(u) = u$ and the Neumann condition is $\mathcal{N}_{Poisson}(u) = \partial_n u$. To design optimized Schwarz methods, we only need to consider Robin conditions on the interface, which are a linear combination of the Dirichlet and Neumann conditions, i.e. $\partial_n u + pu$. Then the best convergence factor can be obtained by optimizing the parameter p. However, it is more challenging to propose optimized Schwarz methods for the biharmonic problem. According to the discussion above, by setting $\mathcal{D}_2 := \mathcal{D}_1$, we have 4 different pairs of Dirichlet conditions $\mathcal{D}_j$ and Neumann conditions $\mathcal{N}_j$, $(j = 1, 2, 3, 4)$. The corresponding Robin conditions are $\mathcal{N}_j(u) + P_j\mathcal{D}_j(u)$, where P_j is a 2×2 matrix rather than a single parameter. Optimizing the matrix P_j for each Robin condition is technical, as we will see later in this paper.

We are interested here in fully understanding classical and optimized Schwarz methods for the biharmonic problem, because the performance of these methods depends on what one chooses as the Dirichlet and the Neumann condition. Our results are based on an observation in the short conference paper [10] that classical Schwarz methods can converge much better than observed in the literature depending on this choice, and the choice also influences optimized Schwarz methods. We provide here a comprehensive numerical analysis for these methods, prove the results that were announced in [10] without proofs, give convergence rate estimates, show well-posedness for subdomain problems, give a detailed study of the choice of the Robin parameter matrices, and also present extensive numerical experiments, including as application the Golden Gate Bridge.

In Section 2, we introduce the family of classical Schwarz methods and their corresponding convergence factors. In Section 3, a new family of optimized Schwarz methods are proposed. We then give a precise convergence analysis for the members of the family, and compare their convergence rates. All the convergence analyses are based on an unbounded domain decomposed into two half-planes. We show numerical results in Section 4 to illustrate our analysis, and draw conclusions in Section 5.

2. Three Classical Schwarz Algorithms. We simplify the presentation and analysis by considering the biharmonic equation on an unbounded domain,

$$\Delta^2 u = f \quad \text{in } \Omega := \mathbb{R}^2, \tag{2.1}$$

and we assume that $f \neq 0$ only in a bounded domain and u decays at infinity. Let the radius $r := (x^2 + y^2)^{\frac{1}{2}}$ and the domain $\Omega_0 := r < a$, then we know that $f = 0$ in the unbounded domain $\Omega \backslash \Omega_0$ for sufficient large a. Note that the problem in Ω_0 is well-posed with some suitable boundary condition, so we only need to consider the far field solution in $\Omega\backslash\Omega_0$. Actually, for the Laplace equation $-\Delta u = 0$ in $\Omega\backslash\Omega_0$, we know that it is well-posed with u decays at infinity, and its solution in polar coordinates is of the form $u(r,\varphi) = \sum_{m=1}^{\infty} \frac{1}{r^m}(A_m \cos(m\varphi) + B_m \sin(m\varphi))$, where A_m and B_m are constants dependent of the boundary condition on $r = a$. Furthermore, the solution to $-\Delta u = \frac{1}{r^m}\cos(m\varphi)$ and $-\Delta u = \frac{1}{r^m}\sin(m\varphi)$, $m \geqslant 3$ with u decays at infinity in $\Omega\backslash\Omega_0$ are $u(r,\varphi) = -\frac{1}{4(m-1)r^{m-2}}\cos(m\varphi)$ and $u(r,\varphi) = -\frac{1}{4(m-1)r^{m-2}}\sin(m\varphi)$. By the observation that $\Delta^2 u = -\Delta(-\Delta u)$, we obtain the problem (2.1) is well-posed, with the solution of the form $u = \sum_{m=1}^{\infty} \frac{1}{r^m}(A_m \cos(m\varphi) + B_m \sin(m\varphi)) + \sum_{m=3}^{\infty} \frac{1}{r^{m-2}}(C_m \cos(m\varphi) + D_m \sin(m\varphi))$ for large r. Let Ω be divided into two subdomains $\Omega_1 = (-\infty, L) \times \mathbb{R}$ and $\Omega_2 = (0, +\infty) \times \mathbb{R}$ with overlap $L \geqslant 0$. More general decompositions are considered in Section 4. The interface for subdomain Ω_1, which is $x = L$, is denoted by Γ_1, and for subdomain Ω_2, its interface at $x = 0$ is denoted by Γ_2. We denote by n_i, $i = 1, 2$ the unit outward normal vector of Ω_i on Γ_i, and by τ_i the corresponding tangential vector along Γ_i, which implies that $n_1 = -n_2$ and $\tau_1 = -\tau_2$. Let $f_1 := f|_{\Omega_1}, f_2 := f|_{\Omega_2}$. We can then define three different Schwarz algorithms by just using the indices $j = 1, 3, 4$:

Classical Schwarz algorithm CS_j: for a given initial guess

$$\mathbf{g}_1^0 = \begin{bmatrix} g_{1A}^0 \\ g_{1B}^0 \end{bmatrix},$$

CS_j performs for iteration index $n = 0, 1, 2, \ldots$ the steps[1]:

1. Compute in Ω_1 an approximate solution u_1^n by solving the Dirichlet problem

$$\Delta^2 u_1^n = f_1 \quad \text{in } \Omega_1, \quad \mathcal{D}_j(u_1^n) = \mathbf{g}_1^n \quad \text{on } \Gamma_1. \tag{2.2}$$

2. Update the transmission condition for Ω_2 by setting $\mathbf{g}_2^n = \mathcal{D}_j(u_1^n)$.
3. Compute in Ω_2 an approximate solution u_2^n by solving the Dirichlet problem

$$\Delta^2 u_2^n = f_2 \quad \text{in } \Omega_2, \quad \mathcal{D}_j(u_2^n) = \mathbf{g}_2^n \quad \text{on } \Gamma_2. \tag{2.3}$$

4. Update the transmission condition for Ω_1 by setting $\mathbf{g}_1^{n+1} = \mathcal{D}_j(u_2^n)$.

To compare the different Schwarz methods, we need to study their contraction properties. Note that the solution u of (2.1) is a fixed point for each method, and by linearity, it is sufficient to study the error equations, i.e. $f = 0$, and to analyze convergence to zero. Let $u_i (i = 1, 2)$ be the solution of (2.2) and (2.3) with $f_i = 0$ and the corresponding boundary condition $\mathcal{D}_j(u_i) = \mathbf{g}_i = [g_{iA}\ g_{iB}]^T$ on Γ_i. As in [7] for Schwarz methods applied to Laplace problem, we take a Fourier transform in the y direction, which transforms $u_i(x,y)$, $g_{iA}(y)$, $g_{iB}(y)$ into $\widehat{u}_i = \widehat{u}_i(x,k)$, $\widehat{g}_{iA} = \widehat{g}_{iA}(k)$ and $\widehat{g}_{iB} = \widehat{g}_{iB}(k)$, $k \neq 0$ denoting the Fourier parameter[2], and we obtain the subdomain ordinary differential equations (ODEs)

$$\frac{\partial^4 \widehat{u}_1}{\partial x^4} - 2k^2 \frac{\partial^2 \widehat{u}_1}{\partial x^2} + k^4 \widehat{u}_1 = 0, \quad x \leqslant L, \qquad \frac{\partial^4 \widehat{u}_2}{\partial x^4} - 2k^2 \frac{\partial^2 \widehat{u}_2}{\partial x^2} + k^4 \widehat{u}_2 = 0, \quad x \geqslant 0. \tag{2.4}$$

[1]This n has no relation to the n in the normal derivative ∂_n.
[2]The constant mode $k = 0$ is excluded because we assume that solutions decay at infinity to zero.

To solve these ODEs, we need the solutions of the characteristic equation $\lambda^4 - 2k^2\lambda^2 + k^4 = 0$, i.e. $\lambda = \pm k$. The general solution on subdomain Ω_i, $i = 1, 2$, is thus given by

$$\widehat{u}_i(x,k) = C_1 e^{|k|x} + \widetilde{C}_1 x e^{|k|x} + C_2 e^{-|k|x} + \widetilde{C}_2 x e^{-|k|x}.$$

By assumption the solutions u_i decay at infinity, and hence the constants corresponding to the growing solutions must be zero, yielding

$$\widehat{u}_1(x,k) = C_1 e^{|k|x} + \widetilde{C}_1 x e^{|k|x}, \quad x \leqslant L, \quad \widehat{u}_2(x,k) = C_2 e^{-|k|x} + \widetilde{C}_2 x e^{-|k|x}, \quad x \geqslant 0. \tag{2.5}$$

All classical Schwarz algorithms CS_j, $j = 1, 3, 4$ have subdomain iterates of this form; their convergence is determined by how the constants C_1, $\widetilde{C}_1$, C_2 and $\widetilde{C}_2$ are affected by the iteration of CS_j. Note that when $L = 0$, which is the non overlapping case, the interface condition $\mathbf{g}_1^n$ will not change during the iteration procedure. This means the classical Schwarz methods do not converge in the non overlapping case, so we only consider the overlapping case, i.e. $L > 0$ in the following analysis in this section.

2.1. Analysis of CS_1. If we introduce the subdomain solution (2.5) at iteration step n into the Dirichlet transmission condition of step 1 of CS_1 in (2.2), we obtain

$$\begin{bmatrix} \widehat{u}_1^n(x_1,k) \\ \partial_{n_1}\widehat{u}_1^n(x_1,k) \end{bmatrix} = \begin{bmatrix} C_1^n e^{|k|x_1} + \widetilde{C}_1^n x_1 e^{|k|x_1} \\ C_1^n |k| e^{|k|x_1} + \widetilde{C}_1^n (e^{|k|x_1} + |k| x_1 e^{|k|x_1}) \end{bmatrix} = \begin{bmatrix} \widehat{g}_{1A}^n \\ \widehat{g}_{1B}^n \end{bmatrix} \quad \text{on } \Gamma_1, \tag{2.6}$$

where $x = x_1 = L$ is the interface Γ_1. Using step 2 in the transmission condition for Ω_2 on the interface Γ_2 leads to

$$\begin{bmatrix} \widehat{g}_{2A}^n \\ \widehat{g}_{2B}^n \end{bmatrix} = \begin{bmatrix} \widehat{u}_1^n(x_2,k) \\ \partial_{n_2}\widehat{u}_1^n(x_2,k) \end{bmatrix} = \begin{bmatrix} C_1^n e^{|k|x_2} + \widetilde{C}_1^n x_2 e^{|k|x_2} \\ -C_1^n |k| e^{|k|x_2} - \widetilde{C}_1^n (e^{|k|x_2} + |k| x_2 e^{|k|x_2}) \end{bmatrix} \quad \text{on } \Gamma_2, \tag{2.7}$$

where $x = x_2 = 0$ is the interface Γ_2. To simplify the notation, we now introduce the vectors

$$\bar{\mathbf{c}}_i^n := \begin{bmatrix} C_i^n \\ \widetilde{C}_i^n \end{bmatrix}, \quad \bar{\mathbf{g}}_i^n := \begin{bmatrix} \widehat{g}_{iA}^n \\ \widehat{g}_{iB}^n \end{bmatrix},$$

and the matrices

$$A_1 := e^{|k|x_1} \begin{bmatrix} 1 & x_1 \\ |k| & 1 + |k|x_1 \end{bmatrix}, \quad T_1 := e^{|k|x_2} \begin{bmatrix} 1 & x_2 \\ -|k| & -1 - |k|x_2 \end{bmatrix}.$$

We can then write (2.6) and (2.7) in compact form, $A_1\bar{\mathbf{c}}_1^n = \bar{\mathbf{g}}_1^n$, and $T_1\bar{\mathbf{c}}_1^n = \bar{\mathbf{g}}_2^n$. Similarly, we obtain for the subproblem in Ω_2 the matrices

$$A_2 := e^{-|k|x_2} \begin{bmatrix} 1 & x_2 \\ |k| & -1 + |k|x_2 \end{bmatrix}, \quad T_2 := e^{-|k|x_1} \begin{bmatrix} 1 & x_1 \\ -|k| & 1 - |k|x_1 \end{bmatrix}.$$

The classical Schwarz algorithm CS_1 can thus be written in Fourier in the form

$$A_1\bar{\mathbf{c}}_1^n = \bar{\mathbf{g}}_1^n, \quad T_1\bar{\mathbf{c}}_1^n = \bar{\mathbf{g}}_2^n, \qquad A_2\bar{\mathbf{c}}_2^n = \bar{\mathbf{g}}_2^n, \quad T_2\bar{\mathbf{c}}_2^n = \bar{\mathbf{g}}_1^{n+1}.$$

By eliminating the intermediate variables $\bar{\mathbf{g}}_2^n$, we obtain on the interface Γ_1

$$\bar{\mathbf{g}}_1^{n+1} = T_2 A_2^{-1} T_1 A_1^{-1} \bar{\mathbf{g}}_1^n. \tag{2.8}$$

In order to study the convergence factor of CS_1, we have to compute for each Fourier mode $k \neq 0$ the eigenvalues of the iteration matrix $T_2A_2^{-1}T_1A_1^{-1}$. Since $x_1 - x_2 = L$, we obtain by a direct calculation

$$T_2A_2^{-1}T_1A_1^{-1} = -e^{-2|k|L}\begin{bmatrix} |k|L+1 & -L \\ -|k|^2L & |k|L-1 \end{bmatrix}^2,$$

where in this continues case with unbounded domain, $|k| \in [0, \infty)$. In a numerical context, the Fourier frequencies $|k|$ are contained in $[k_{\min}, k_{\max}]$ with $k_{\min}, k_{\max} > 0$. This is because in practice, the computational domain is bounded, say with interface length a constant C, which leads to $k_{\min} \sim \frac{1}{C}$, a constant. On the other hand, the mesh size is h, which makes the largest frequency $k_{\max} \sim \frac{1}{h}$. Then we obtain (see also [17]):

THEOREM 2.1. *If $L > 0$, the convergence factor ρ_{CS_1} for the algorithm CS_1 is*

$$\rho_{CS_1}(L) = (k_{\min}L + \sqrt{k_{\min}^2L^2+1})^2e^{-2k_{\min}L} = 1 - \frac{1}{3}k_{\min}^3L^3 + O(L^5).$$

Proof. By a direct calculation, we obtain for the eigenvalues of $T_2A_2^{-1}T_1A_1^{-1}$

$$\lambda = \{-(|k|L + \sqrt{|k|^2L^2+1})^2e^{-2|k|L}, -(|k|L - \sqrt{|k|^2L^2+1})^2e^{-2|k|L}\}.$$

Then the convergence factor ρ_{CS_1} is

$$\begin{aligned}\rho_{CS_1} &= \max_{|k|_{\min}\leqslant|k|\leqslant|k|_{\max}} \max\{(|k|L + \sqrt{|k|^2L^2+1})^2e^{-2|k|L}, (|k|L - \sqrt{|k|^2L^2+1})^2e^{-2|k|L}\} \\ &= \max_{|k|_{\min}\leqslant|k|\leqslant|k|_{\max}} (|k|L + \sqrt{|k|^2L^2+1})^2e^{-2|k|L} = (k_{\min}L + \sqrt{k_{\min}^2L^2+1})^2e^{-2k_{\min}L}.\end{aligned}$$

The last equation comes from the fact that function $w(x) := (x + \sqrt{x^2+1})^2e^{-2x}$ is monotonically decreasing for all $x > 0$. Then the proof is concluded by a Taylor expansion. ∎

The classical Dirichlet transmission condition (1.2) thus leads to a convergence factor $1-O(L^3)$, in contrast to the Laplace case with linear dependence $1-O(L)$, the latter being much better when the overlap L is small.

2.2. Analysis of CS_3 and CS_4 . For the other two possible Dirichlet conditions in (1.5) and (1.6), the convergence factor only depends linearly on L:

THEOREM 2.2. *If $L > 0$, the convergence factors for the algorithms CS_3 and CS_4 are the same,*

$$\rho_{CS_{34}}(L) = e^{-2k_{\min}L} = 1 - 2k_{\min}L + O(L^2). \tag{2.9}$$

Proof. Similar as in the analysis for CS_1, we obtain the corresponding matrices for CS_3 ($\sigma = 1$) and CS_4 ($-1 < \sigma < 1$),

$$A_1 := e^{|k|x_1}\begin{bmatrix} 1 & x_1 \\ (1-\sigma)|k|^2 & (1-\sigma)|k|^2x_1+2|k| \end{bmatrix},\ T_1 := e^{|k|x_2}\begin{bmatrix} 1 & x_2 \\ (1-\sigma)|k|^2 & (1-\sigma)|k|^2x_2+2|k| \end{bmatrix},$$

$$A_2 := e^{-|k|x_2}\begin{bmatrix} 1 & x_2 \\ (1-\sigma)|k|^2 & (1-\sigma)|k|^2x_2-2|k| \end{bmatrix},\ T_2 := e^{-|k|x_1}\begin{bmatrix} 1 & x_1 \\ (1-\sigma)|k|^2 & (1-\sigma)|k|^2x_1-2|k| \end{bmatrix}.$$

Then by a direct calculation, we obtain for the iteration matrix

$$T_2A_2^{-1}T_1A_1^{-1} = -\frac{e^{-2|k|L}}{4|k|^2}\begin{bmatrix} (1-\sigma)|k|^2L+2|k| & -L \\ (1-\sigma)^2|k|^4L & -(1-\sigma)|k|^2L+2|k| \end{bmatrix}^2,$$

which has two identical eigenvalues $\lambda_{12} = -e^{-2|k|L}$, leading to (2.9). ∎

Comparing with CS_1, this is a substantially improved convergence factor, which is now as good as the Schwarz method for Laplace's equation [7].

3. Four Optimized Schwarz Algorithms. Optimized Schwarz methods [7] combine the Dirichlet and Neumann conditions in their transmission conditions. To simplify the notation, we also introduce the redundant operator $\mathcal{D}_2 := \mathcal{D}_1$, and thus obtain four different optimized Schwarz algorithms using the indices $j = 1, 2, 3, 4$:

Optimized Schwarz algorithm OS_j: for a given initial guess

$$\mathbf{g}_1^0 = \begin{bmatrix} g_{1A}^0 \\ g_{1B}^0 \end{bmatrix},$$

and iteration index $n = 0, 1, 2, \ldots$, OS_j performs the steps:

1. Compute in Ω_1 an approximate solution u_1^n by solving the Robin problem

$$\Delta^2 u_1^n = f_1 \quad \text{in } \Omega_1, \quad (\mathcal{N}_j + P_j\mathcal{D}_j)(u_1^n) = \mathbf{g}_1^n \quad \text{on } \Gamma_1, \tag{3.1}$$

   where P_j is a two by two matrix containing four adjustable parameters.
2. Update the transmission condition for Ω_2 by setting $\mathbf{g}_2^n = (\mathcal{N}_j + P_j\mathcal{D}_j)(u_1^n)$.
3. Compute in Ω_2 an approximate solution u_2^n by solving the Robin problem

$$\Delta^2 u_2^n = f_2 \quad \text{in } \Omega_2, \quad (\mathcal{N}_j + P_j\mathcal{D}_j)(u_2^n) = \mathbf{g}_2^n \quad \text{on } \Gamma_2. \tag{3.2}$$

4. Update the transmission condition for Ω_1 by setting $\mathbf{g}_1^{n+1} = (\mathcal{N}_j + P_j\mathcal{D}_j)(u_2^n)$.

Choosing P_j is technical, since we need to ensure well-posedness of each subproblem and also optimize convergence. To find the optimal choice for P_j, Fourier analysis as in Section 2 leads for OS_1 ($\sigma = 1$) and OS_2 ($-1 < \sigma < 1$) to the matrices

$$\begin{aligned}
A_1 &:= e^{|k|x_1}\begin{bmatrix} (1-\sigma)|k|^2 & 2|k| + (1-\sigma)|k|^2x_1 \\ (1-\sigma)|k|^3 & -(1+\sigma)|k|^2 + (1-\sigma)|k|^3x_1 \end{bmatrix} + P_je^{|k|x_1}\begin{bmatrix} 1 & x_1 \\ |k| & 1+|k|x_1 \end{bmatrix},\\
T_1 &:= e^{|k|x_2}\begin{bmatrix} (1-\sigma)|k|^2 & 2|k| + (1-\sigma)|k|^2x_2 \\ -(1-\sigma)|k|^3 & (1+\sigma)|k|^2 - (1-\sigma)|k|^3x_2 \end{bmatrix} + P_je^{|k|x_2}\begin{bmatrix} 1 & x_2 \\ -|k| & -1-|k|x_2 \end{bmatrix},\\
A_2 &:= e^{-|k|x_2}\begin{bmatrix} (1-\sigma)|k|^2 & -2|k| + (1-\sigma)|k|^2x_2 \\ (1-\sigma)|k|^3 & (1+\sigma)|k|^2 + (1-\sigma)|k|^3x_2 \end{bmatrix} + P_je^{-|k|x_2}\begin{bmatrix} 1 & x_2 \\ |k| & -1+|k|x_2 \end{bmatrix},\\
T_2 &:= e^{-|k|x_1}\begin{bmatrix} (1-\sigma)|k|^2 & -2|k| + (1-\sigma)|k|^2x_1 \\ -(1-\sigma)|k|^3 & -(1+\sigma)|k|^2 - (1-\sigma)|k|^3x_1 \end{bmatrix} + P_je^{-|k|x_1}\begin{bmatrix} 1 & x_1 \\ -|k| & 1-|k|x_1 \end{bmatrix}.
\end{aligned}$$

We still have the iteration formula (2.8). To make $\bar{\mathbf{g}}_1^n$ going to 0 as fast as possible, the optimal choice of P_j is determined by setting $T_1 = 0$ or $T_2 = 0$, and we obtain by a lengthy but not difficult calculation the compact and elegant result

$$P_1 = P_2 = \begin{bmatrix} (1+\sigma)|k|^2 & 2|k| \\ 2|k|^3 & (1+\sigma)|k|^2 \end{bmatrix}. \tag{3.3}$$

Similarly, the matrices for OS_3 ($\sigma = 1$) and OS_4 ($-1 < \sigma < 1$) are

$$A_1 := e^{|k|x_1}\begin{bmatrix} |k| & 1+|k|x_1 \\ (1-\sigma)|k|^3 & -(1+\sigma)|k|^2+(1-\sigma)|k|^3x_1 \end{bmatrix} + P_j e^{|k|x_1}\begin{bmatrix} 1 & x_1 \\ (1-\sigma)|k|^2 & 2|k|+(1-\sigma)|k|^2x_1 \end{bmatrix},$$
$$T_1 := e^{|k|x_2}\begin{bmatrix} -|k| & -1-|k|x_2 \\ -(1-\sigma)|k|^3 & (1+\sigma)|k|^2-(1-\sigma)|k|^3x_2 \end{bmatrix} + P_j e^{|k|x_2}\begin{bmatrix} 1 & x_2 \\ (1-\sigma)|k|^2 & 2|k|+(1-\sigma)|k|^2x_2 \end{bmatrix},$$
$$A_2 := e^{-|k|x_2}\begin{bmatrix} |k| & -1+|k|x_2 \\ (1-\sigma)|k|^3 & (1+\sigma)|k|^2+(1-\sigma)|k|^3x_2 \end{bmatrix} + P_j e^{-|k|x_2}\begin{bmatrix} 1 & x_2 \\ (1-\sigma)|k|^2 & -2|k|+(1-\sigma)|k|^2x_2 \end{bmatrix},$$
$$T_2 := e^{-|k|x_1}\begin{bmatrix} -|k| & 1-|k|x_1 \\ -(1-\sigma)|k|^3 & -(1+\sigma)|k|^2-(1-\sigma)|k|^3x_1 \end{bmatrix} + P_j e^{-|k|x_1}\begin{bmatrix} 1 & x_1 \\ (1-\sigma)|k|^2 & -2|k|+(1-\sigma)|k|^2x_1 \end{bmatrix}.$$

The optimal choice of P_j leading to $T_1 = 0$ or $T_2 = 0$ is then

$$P_3 = P_4 = \begin{bmatrix} \frac{1}{2}(1+\sigma)|k| & \frac{1}{2|k|} \\ \frac{1}{2}(1-\sigma)(\sigma+3)|k|^3 & -\frac{1}{2}(1+\sigma)|k| \end{bmatrix}. \tag{3.4}$$

The optimal choices of P_j in (3.3) and (3.4) depend on the frequency $|k|$, which corresponds to a non-local operator (see [7] page 703 for details). A local, structurally consistent constant approximation is obtained[3] by replacing $|k|$ by a constant $p \geqslant 0$, which leads to

$$P_1^a = P_2^a = \begin{bmatrix} (1+\sigma)p^2 & 2p \\ 2p^3 & (1+\sigma)p^2 \end{bmatrix}, \quad P_3^a = P_4^a = \begin{bmatrix} \frac{1}{2}(1+\sigma)p & \frac{1}{2p} \\ \frac{1}{2}(1-\sigma)(\sigma+3)p^3 & -\frac{1}{2}(1+\sigma)p \end{bmatrix}. \tag{3.5}$$

3.1. Analysis of OS_1 and OS_3 . To analyze the convergence rate, we still need to estimate the eigenvalues of the iteration matrix (2.8).

THEOREM 3.1. *For OS_1 and OS_3, i.e. $\sigma = 1$ in (3.5), which leads to*

$$P_1^a = \begin{bmatrix} 2p^2 & 2p \\ 2p^3 & 2p^2 \end{bmatrix}, \quad P_3^a = \begin{bmatrix} p & \frac{1}{2p} \\ 0 & -p \end{bmatrix}, \tag{3.6}$$

the convergence factor becomes the one for the Laplace problem,

$$\left(\frac{p-|k|}{p+|k|}\right)^2 e^{-2|k|L} < 1. \tag{3.7}$$

In the case with overlap, $L > 0$, we obtain for small overlap L the best choice of p and the corresponding convergence factor as

$$p \sim \left(\frac{k_{\min}^2}{2L}\right)^{\frac{1}{3}}, \quad \rho_{OS_{13}}(L) = 1 - 4(2k_{\min})^{\frac{1}{3}}L^{\frac{1}{3}} + O(L^{\frac{2}{3}}). \tag{3.8}$$

Here $k_{\min}$ denotes the smallest frequency along the interface and "$\sim$" means $p = O(L^{-\frac{1}{3}})$ when $L \to 0$. Without overlap, $L = 0$, we get, with $k_{\max}$ the largest frequency along the interface, the best choice of p and the corresponding convergence factor as

$$p = \sqrt{k_{\min}k_{\max}}, \; \rho_{OS_{13}}(0) = \left(\frac{\sqrt{k_{\max}}-\sqrt{k_{\min}}}{\sqrt{k_{\max}}+\sqrt{k_{\min}}}\right)^2 = 1 - 4\sqrt{\frac{k_{\min}}{k_{\max}}} + O\left(\frac{1}{k_{\max}}\right). \tag{3.9}$$

[3]This is a fundamentally new and important idea to find good constant approximations in this complex setting, which is similar as the "zeroth order optimized transmission conditions" in [7] for the Poisson problem. We can also approximate it with a higher order ik-polynomial, which is future work.

Proof. By a direct calculation, we see that for (2.8), $T_2A_2^{-1} = T_1A_1^{-1}$ always holds both for OS_1 and OS_3. So we only need to estimate the eigenvalues of $T_1A_1^{-1}$, which is a 2×2 matrix. A simple calculation shows that for both OS_1 and OS_3, the two eigenvalues are the same and coincide, $\lambda_{12}(T_1A_1^{-1}) = -\frac{|k|-p}{|k|+p}e^{-|k|L}$, which leads to (3.7). Following the same analysis in [7], we thus obtain (3.8) and (3.9). ∎

3.2. Analysis of OS_2 and OS_4 . For the OS_2 and OS_4 methods, things become different and the convergence rate we obtain is worse than for the OS_1 and OS_3 methods.

THEOREM 3.2. *For OS_2 and OS_4, i.e. $-1 < \sigma < 1$ in (3.5), which leads to*

(3.10)
$$P_2^a = \begin{bmatrix} (1+\sigma)p^2 & 2p \\ 2p^3 & (1+\sigma)p^2 \end{bmatrix}, \quad P_4^a = \begin{bmatrix} \frac{1}{2}(1+\sigma)p & \frac{1}{2p} \\ \frac{1}{2}(1-\sigma)(\sigma+3)p^3 & -\frac{1}{2}(1+\sigma)p \end{bmatrix},$$

the asymptotic behavior of the best choice of p and the corresponding convergence factor, with overlap $L > 0$ small is

(3.11)
$$p \sim 2^{-\frac{8}{15}} \left(\frac{12k_{\min}^4}{(1-\sigma^2)L}\right)^{\frac{1}{5}}, \ \rho_{OS_{24}}(L) = 1 - \frac{32}{(1-\sigma)(\sigma+3)} \cdot \left(\frac{(1-\sigma^2)k_{\min}}{6}\right)^{\frac{3}{5}} L^{\frac{3}{5}} + O(L^{\frac{4}{5}}).$$

Without overlap, $L = 0$, the asymptotic behavior of the best choice of p and the corresponding convergence factor for $k_{\max}$ large is

$$p \sim \sqrt{k_{\min}k_{\max}}, \quad \rho_{OS_{24}}(0) = 1 - \frac{16k_{\min}^{\frac{3}{2}}}{3-2\sigma-\sigma^2}\frac{1}{k_{\max}^{\frac{3}{2}}} + O\left(\frac{1}{k_{\max}^{\frac{5}{2}}}\right). \tag{3.12}$$

In practical applications, the overlap L is usually an integer times the mesh size h. Since $h \sim \frac{1}{k_{\max}}$, the asymptotic behavior for large $k_{\max}$ represents the corresponding convergence factor as the mesh is refined. To prove this theorem, we need several lemmas.

LEMMA 3.3. *Let $a := 1 - \sigma \in (0, 2)$, $b := \sigma + 3 \in (2, 4)$, and*

(3.13)
$$\lambda_1(L) := \frac{1}{4p|k| + ab(|k|-p)^2}\Big(4p|k| + a(a|k|^2 + bp^2)|k|L + [a^2(a|k|^2 + bp^2)^2|k|^2L^2 + 8a(a|k|^2 + bp^2)|k|^2pL + ab(a|k|^2 + bp^2)(b|k|^2 + ap^2)]^{\frac{1}{2}}\Big)\frac{|k|-p}{|k|+p}e^{-|k|L}.$$

Then by choosing the parameters to be (3.10), where $-1 < \sigma < 1$, the convergence factor of OS_2 and OS_4 is

$$\rho = |\lambda_1|^2.$$

Proof. As in the analysis of Theorem 3.1, we find that $T_2A_2^{-1} = T_1A_1^{-1}$ always holds both for OS_2 and OS_4. So it is sufficient to estimate the eigenvalues of $T_1A_1^{-1}$, which is again a 2×2 matrix. A simple calculation shows that the eigenvalues of OS_2 and OS_4 are the same, but now we have two distinct eigenvalues,

$$\lambda_{12}(T_1A_1^{-1}) = \frac{1}{4p|k| + ab(|k|-p)^2}\Big(4p|k| + a(a|k|^2 + bp^2)|k|L \pm [a^2(a|k|^2 + bp^2)^2|k|^2L^2 + 8a(a|k|^2 + bp^2)|k|^2pL + ab(a|k|^2 + bp^2)(b|k|^2 + ap^2)]^{\frac{1}{2}}\Big)\frac{|k|-p}{|k|+p}e^{-|k|L}.$$

The contraction factor is thus the larger of the two eigenvalues in modulus squared, which is, $\rho = |\lambda_1|^2$. ∎

Note that ρ is also a function of L. Then we consider the nonoverlapping case first, i.e. $L = 0$.

LEMMA 3.4. *For the nonoverlapping case, the best choice is* $p = \sqrt{k_{\min} k_{\max}}$, *and the corresponding convergence factor is*

$$\rho(0) = 1 - \frac{16}{(1-\sigma)(\sigma+3)} \frac{k_{\min}^{\frac{3}{2}}}{k_{\max}^{\frac{3}{2}}} + O(k_{\max}^{-\frac{5}{2}}).$$

Proof. Let $L = 0$, then (3.13) simplifies to

$$\lambda_1^{nov} := \lambda_1(0) = \frac{4p|k| + [ab(a|k|^2 + bp^2)(b|k|^2 + ap^2)]^{\frac{1}{2}}}{4p|k| + ab(|k|-p)^2} \frac{|k|-p}{|k|+p}. \tag{3.14}$$

Now for any fixed $|k|$, by a direct computation, noticing that $(a-b)^2 < 16$, we have

(3.15) ∎

$$\begin{aligned}
\partial_p \lambda_1^{nov} &= \frac{1}{(|k|+p)(4p|k| + ab(|k|-p)^2)} \Bigg[\Bigg(4|k| + \frac{abp\Big(a(a|k|^2+bp^2) + b(b|k|^2+ap^2)\Big)}{\sqrt{ab(a|k|^2+bp^2)(b|k|^2+ap^2)}} \Bigg)(|k|-p) \\
&- (4p|k| + \sqrt{ab(a|k|^2+bp^2)(b|k|^2+ap^2)}) \Big(1 + \frac{|k|-p}{|k|+p} + \frac{(|k|-p)(4|k| - 2ab(|k|-p))}{4p|k| + ab(|k|-p)^2} \Big) \Bigg] \\
&= \frac{4|k|}{(|k|+p)^2(4p|k| + ab(|k|-p)^2)^2} \\
&\cdot \Bigg[ab(|k|^2+p^2)(|k|-p)^2 \Big(1 - \frac{((|k|-p)^2 + 2|k|p)\sqrt{ab(a|k|^2+bp^2)(b|k|^2+ap^2)}}{(a|k|^2+bp^2)(b|k|^2+ap^2)} \Big) \\
&- 8|k|^2p^2 - 2|k|^2p^2 \frac{((a-b)^2|k|p + 2ab(|k|^2+p^2))\sqrt{ab(a|k|^2+bp^2)(b|k|^2+ap^2)}}{(a|k|^2+bp^2)(b|k|^2+ap^2)} \Bigg] \\
&= \frac{4|k|}{(|k|+p)^2(4p|k| + ab(|k|-p)^2)^2} \\
&\cdot \Bigg[ab(|k|^2+p^2)(|k|-p)^2 \frac{(a-b)^2|k|^2p^2}{\sqrt{(a|k|^2+bp^2)(b|k|^2+ap^2)}\big(\sqrt{(a|k|^2+bp^2)(b|k|^2+ap^2)} + \sqrt{ab}(|k|^2+p^2)\big)} \\
&- 8|k|^2p^2 - 2|k|^2p^2 \frac{((a-b)^2|k|p + 2ab(|k|^2+p^2))\sqrt{ab(a|k|^2+bp^2)(b|k|^2+ap^2)}}{(a|k|^2+bp^2)(b|k|^2+ap^2)} \Bigg] \\
&\leqslant \frac{4|k|}{(|k|+p)^2(4p|k| + ab(|k|-p)^2)^2} \cdot \Bigg[\frac{ab(|k|^2+p^2)(|k|-p)^2 \cdot (a-b)^2|k|^2p^2}{\sqrt{ab}(|k|^2+p^2)\big(\sqrt{ab}(|k|^2+p^2) + \sqrt{ab}(|k|^2+p^2)\big)} \\
&- 8|k|^2p^2 - 2|k|^2p^2 \frac{((a-b)^2|k|p + 2ab(|k|^2+p^2))\sqrt{ab(a|k|^2+bp^2)(b|k|^2+ap^2)}}{(a|k|^2+bp^2)(b|k|^2+ap^2)} \Bigg] \\
&\leqslant \frac{4|k|}{(|k|+p)^2(4p|k| + ab(|k|-p)^2)^2} \cdot \Bigg[\frac{(a-b)^2|k|^2p^2}{2} - 8|k|^2p^2 \\
&- 2|k|^2p^2 \frac{((a-b)^2|k|p + 2ab(|k|^2+p^2))\sqrt{ab(a|k|^2+bp^2)(b|k|^2+ap^2)}}{(a|k|^2+bp^2)(b|k|^2+ap^2)} \Bigg] \\
&< 0.
\end{aligned}$$

So for $p < k_{\min}$, it always holds that $\partial_p \rho = 2\lambda_1^{nov}\partial_p\lambda_1^{nov} < 0$, which shows that the best choice of p lies in $[k_{\min}, +\infty]$. Noticing next that the symbol $|k|$ and p are antisymmetric in (3.14), we have $\partial_{|k|}\lambda_1^{nov} > 0$ for fixed p. So the best choice of p satisfies the equioscillation equation

$$-\lambda_1^{nov}(k_{\min}, p) = \lambda_1^{nov}(k_{\max}, p).$$

By a direct calculation, the solution to this problem is

$$p = \sqrt{k_{\min}k_{\max}},$$

and the corresponding convergence factor without overlap, $L = 0$, is for $k_{\max}$ large

$$\rho(0) = 1 - \frac{16}{(1-\sigma)(\sigma+3)}\frac{k_{\min}^{\frac{3}{2}}}{k_{\max}^{\frac{3}{2}}} + O(k_{\max}^{-\frac{5}{2}}).$$

For the overlapping case, we only give an asymptotic proof, and we divide it into two parts, which are the next two lemmas.

Lemma 3.5. *Fix $p > 0$ and $L > 0$, then there is a maximum $\bar{k}$ in $[k_{\min}, +\infty]$ for λ_1. Assuming that $\bar{k} = C_k L^{-\alpha}$, let $p := C_p L^{-\beta}$, where $\alpha > \beta$, then*

$$\lambda_1 = 1 - \frac{8C_p^3}{abC_k^3}L^{3\alpha-3\beta} - \Big(1 - \frac{a}{b}\Big)C_k L^{1-\alpha} + O(L^{\min\{4\alpha-4\beta, 2-2\alpha, 1-\beta\}}), \tag{3.16}$$

and the maximum of λ_1 is obtained when

$$3\alpha - 3\beta = 1 - \alpha, \quad \textit{and} \quad -3\cdot\frac{8C_p^3}{abC_k^4} + \Big(1 - \frac{a}{b}\Big) = 0. \tag{3.17}$$

Proof. By (3.13), computing the derivative with respect to $|k|$, we get

(3.18)

$$\begin{aligned}
\partial_{|k|}\lambda_1 = {} & \frac{e^{-|k|L}}{(|k|+p)(4p|k| + ab(|k|-p)^2)}\Bigg[\Bigg(4p + a(3a|k|^2 + bp^2)L \\
& + \frac{a^2(a|k|^2+bp^2)(3a|k|^2+bp^2)|k|L^2 + 8a(2a|k|^2+bp^2)|k|pL + ab|k|\Big(a(b|k|^2+ap^2) + b(a|k|^2+bp^2)\Big)}{\sqrt{a^2(a|k|^2+bp^2)^2|k|^2L^2 + 8a(a|k|^2+bp^2)|k|^2pL + ab(a|k|^2+bp^2)(b|k|^2+ap^2)}}\Bigg) \\
& \cdot (|k|-p) + \Big(4p|k| + a(a|k|^2+bp^2)|k|L \\
& + \sqrt{a^2(a|k|^2+bp^2)^2|k|^2L^2 + 8a(a|k|^2+bp^2)|k|^2pL + ab(a|k|^2+bp^2)(b|k|^2+ap^2)}\Big)\Big(1 - \frac{|k|-p}{|k|+p} \\
& - (|k|-p)L - \frac{(|k|-p)(4p + 2ab(|k|-p))}{4p|k| + ab(|k|-p)^2}\Big)\Bigg].
\end{aligned}$$

Note that we already have $\partial_{|k|}\lambda_1^{nov} > 0$ for $L = 0$, and according to (3.18), $\partial_{|k|}\lambda_1$ is continuous for all $|k| > 0, p > 0, L \geqslant 0$. So for fixed p, if $|k| < k_s$ is bounded, there exists a small L_s, such that $\partial_{|k|}\lambda_1 > 0$ for all $L \leqslant L_s$. Furthermore, by (3.18) and a direct calculation, for any fixed $p, L > 0$, an asymptotic analysis leads to that there exists a large k_l, such that $\partial_{|k|}\lambda_1 < 0$ $\forall |k| \geqslant k_l$. Based on this observation, there is a maximum $\bar{k}$ in $[k_{\min}, +\infty]$.

Notice that the maximum is obtain at $|k| = \bar{k} = C_k L^{-\alpha}$, and $p = C_p L^{-\beta}$. To reach the best convergence rate, we need to find the optimal choice of β, and then obtain the corresponding value of α. By direct calculation, we obtain for the various terms

$$\begin{aligned}
4p|k| &= 4C_kC_pL^{-\alpha-\beta},\\
ab(|k|-p)^2 &= abC_k^2L^{-2\alpha} - 2abC_kC_pL^{-\alpha-\beta} + abC_p^2L^{-2\beta},\\
a(a|k|^2+bp^2)|k|L &= a^2C_k^3L^{1-3\alpha} + abC_kC_p^2L^{1-\alpha-2\beta},\\
a^2(a|k|^2+bp^2)^2|k|^2L^2 &= a^4C_k^6L^{2-6\alpha} + a^2b^2C_k^2C_p^4L^{2-2\alpha-4\beta} + 2a^3bC_k^4C_p^2L^{2-4\alpha-2\beta},\\
8a(a|k|^2+bp^2)|k|^2pL &= 8a^2C_k^4C_pL^{1-4\alpha-\beta} + 8abC_k^2C_p^3L^{1-2\alpha-3\beta},\\
ab(a|k|^2+bp^2)(b|k|^2+ap^2) &= a^2b^2C_k^4L^{-4\alpha} + ab(a^2+b^2)C_k^2C_p^2L^{-2\alpha-2\beta} + a^2b^2C_p^4L^{-4\beta}.
\end{aligned}$$

Estimating (3.13) term by term, we obtain by lengthy but not difficult calculations

$$\begin{aligned}
&\frac{4p|k|}{4p|k|+ab(|k|-p)^2} = \frac{4C_p}{abC_k}L^{\alpha-\beta} - \frac{4(4-2ab)C_p^2}{a^2b^2C_k^2}L^{2\alpha-2\beta} + \frac{4(3a^2b^2-16ab+16)C_p^3}{a^3b^3C_k^3}L^{3\alpha-3\beta} + O(L^{4\alpha-4\beta}),\\
&\frac{a(a|k|^2+bp^2)|k|L}{4p|k|+ab(|k|-p)^2} = \frac{aC_k}{b}L^{1-\alpha} + O(L^{1-\beta}),\\
&[a^2(a|k|^2+bp^2)^2|k|^2L^2 + 8a(a|k|^2+bp^2)|k|^2pL + ab(a|k|^2+bp^2)(b|k|^2+ap^2)]^{1/2}\\
&= abC_k^2L^{-2\alpha}\Big[1 + \frac{1}{2}\Big(\frac{a^2C_k^2}{b^2}L^{2-2\alpha} + \frac{C_p^4}{C_k^2}L^{2+2\alpha-4\beta} + \frac{2aC_p^2}{b}L^{2-2\beta} + \frac{8C_p}{b^2}L^{1-\beta}\\
&\quad + \frac{8C_p^3}{abC_k^2}L^{1+2\alpha-3\beta} + \frac{(a^2+b^2)C_p^2}{abC_k^2}L^{2\alpha-2\beta} + \frac{C_p^4}{C_k^4}L^{4\alpha-4\beta}\Big) + O(L^{high})\Big],
\end{aligned}$$

where the high order term $O(L^{high})$ means the order of L is equivalent to the square of the previous term, i.e. $\Big(\frac{a^2C_k^2}{b^2}L^{2-2\alpha} + \frac{C_p^4}{C_k^2}L^{2+2\alpha-4\beta} + \frac{2aC_p^2}{b}L^{2-2\beta} + \frac{8C_p}{b^2}L^{1-\beta} + \frac{8C_p^3}{abC_k^2}L^{1+2\alpha-3\beta} + \frac{(a^2+b^2)C_p^2}{abC_k^2}L^{2\alpha-2\beta} + \frac{C_p^4}{C_k^4}L^{4\alpha-4\beta}\Big)^2$, and we use $O(L^{high})$ for simplicity. Similarly

$$\begin{aligned}
&\frac{[a^2(a|k|^2+bp^2)^2|k|^2L^2 + 8a(a|k|^2+bp^2)|k|^2pL + ab(a|k|^2+bp^2)(b|k|^2+ap^2)]^{1/2}}{4p|k|+ab(|k|-p)^2}\\
&= 1 - \frac{(4-2ab)C_p}{abC_k}L^{\alpha-\beta} + \frac{(2a^2b^2-8ab+16)C_p^2}{a^2b^2C_k^2}L^{2\alpha-2\beta} - \frac{2(2-ab)(4-ab)^2C_p^3}{a^3b^3C_k^3}L^{3\alpha-3\beta}\\
&\quad + O(L^{\min\{4\alpha-4\beta,2-2\alpha,1-\beta\}}).
\end{aligned}$$

By further direct calculations, we then obtain for the remaining two terms

$$\begin{aligned}
\frac{|k|-p}{|k|+p} &= 1 - \frac{2p}{|k|+p} = 1 - \frac{2C_pL^{-\beta}}{C_kL^{-\alpha}+C_pL^{-\beta}}\\
&= 1 - \frac{2C_p}{C_k}L^{\alpha-\beta} + \frac{2C_p^2}{C_k^2}L^{2\alpha-2\beta} - \frac{2C_p^3}{C_k^3}L^{3\alpha-3\beta} + O(L^{4\alpha-4\beta}),\\
e^{-|k|L} &= 1 - C_kL^{1-\alpha} + O(L^{2-2\alpha}).
\end{aligned}$$

So the eigenvalue (3.13) can be written asymptotically after a lengthy calculation as

$$\lambda_1 = 1 - \frac{8C_p^3}{abC_k^3}L^{3\alpha-3\beta} - \Big(1-\frac{a}{b}\Big)C_kL^{1-\alpha} + O(L^{\min\{4\alpha-4\beta,2-2\alpha,1-\beta\}}),$$

which is (3.16). Note that $a = 1 - \sigma, b = \sigma + 3$, and since $-1 < \sigma < 1$, we have $(1 - \frac{a}{b})C_k > 0$. Hence for fixed p, i.e. fixed C_p and β, the maximum of λ_1 is obtained when

$$3\alpha - 3\beta = 1 - \alpha, \quad \text{and} \quad -3 \cdot \frac{8C_p^3}{abC_k^4} + \Big(1 - \frac{a}{b}\Big) = 0.$$

∎

LEMMA 3.6. *Assume that $k = k_{\min}$, and also $p = C_p L^{-\beta}$, then*

$$\lambda_1 = -\Big(1 - \frac{8k_{\min}^3}{abC_p^3} L^{3\beta}\Big) + O(L^{\min\{4\beta,2\}}). \tag{3.19}$$

Proof. By a direct calculation, we obtain for the various terms

$$\begin{aligned}
4p|k| &= 4k_{\min} C_p L^{-\beta},\\
ab(|k| - p)^2 &= abk_{\min}^2 - 2abk_{\min} C_p L^{-\beta} + abC_p^2 L^{-2\beta},\\
a(a|k|^2 + bp^2)|k|L &= a^2 k_{\min}^3 L + abk_{\min} C_p^2 L^{1-2\beta},\\
a^2(a|k|^2 + bp^2)^2|k|^2 L^2 &= a^4 k_{\min}^6 L^2 + a^2 b^2 k_{\min}^2 C_p^4 L^{2-4\beta} + 2a^3 b k_{\min}^4 C_p^2 L^{2-2\beta},\\
8a(a|k|^2 + bp^2)|k|^2 pL &= 8a^2 k_{\min}^4 C_p L^{1-\beta} + 8abk_{\min}^2 C_p^3 L^{1-3\beta},\\
ab(a|k|^2 + bp^2)(b|k|^2 + ap^2) &= a^2 b^2 k_{\min}^4 + ab(a^2 + b^2) k_{\min}^2 C_p^2 L^{-2\beta} + a^2 b^2 C_p^4 L^{-4\beta}.
\end{aligned}$$

As before, we estimate (3.13) term by term, and obtain

$$\frac{4p|k|}{4p|k| + ab(|k| - p)^2} = \frac{4k_{\min}}{abC_p} L^{\beta} - \frac{4(4 - 2ab)k_{\min}^2}{a^2 b^2 C_p^2} L^{2\beta} + \frac{4(3a^2 b^2 - 16ab + 16)k_{\min}^3}{a^3 b^3 C_p^3} L^{3\beta} + O(L^{4\beta})$$

$$\frac{a(a|k|^2 + bp^2)|k|L}{4p|k| + ab(|k| - p)^2} = k_{\min} L - \frac{(4 - 2ab)k_{\min}^2}{abC_p} L^{1+\beta} + O(L^{1+2\beta})$$

$$\begin{aligned}
&[a^2(a|k|^2 + bp^2)^2|k|^2 L^2 + 8a(a|k|^2 + bp^2)|k|^2 pL + ab(a|k|^2 + bp^2)(b|k|^2 + ap^2)]^{1/2}\\
&= abC_p^2 L^{-2\beta}\Big[1 + \frac{1}{2}\Big(\frac{a^2 k_{\min}^6}{b^2 C_p^4} L^{2+4\beta} + k_{\min}^2 L^2 + \frac{2ak_{\min}^4}{bC_p^2} L^{2+2\beta} + \frac{8k_{\min}^4}{b^2 C_p^3} L^{1+3\beta} + \frac{8k_{\min}^2}{abC_p} L^{1+\beta}\\
&\qquad + \frac{k_{\min}^4}{C_p^4} L^{4\beta} + \frac{(a^2 + b^2)k_{\min}^2}{abC_p^2} L^{2\beta}\Big) + O(L^{high})\Big],
\end{aligned}$$

$$\begin{aligned}
&\frac{[a^2(a|k|^2 + bp^2)^2|k|^2 L^2 + 8a(a|k|^2 + bp^2)|k|^2 pL + ab(a|k|^2 + bp^2)(b|k|^2 + ap^2)]^{1/2}}{4p|k| + ab(|k| - p)^2}\\
&= 1 - \frac{(4 - 2ab)k_{\min}}{abC_p} L^{\beta} + \frac{(2a^2 b^2 - 8ab + 16)k_{\min}^2}{a^2 b^2 C_p^2} L^{2\beta} - \frac{2(2 - ab)(4 - ab)^2 k_{\min}^3}{a^3 b^3 C_p^3} L^{3\beta}\\
&\qquad + \frac{4k_{\min}^2}{abC_p} L^{1+\beta} + O(L^{\min\{4\beta,2\}}).
\end{aligned}$$

A direct calculation shows that for the remaining terms

$$\begin{aligned}
\frac{|k| - p}{|k| + p} &= -\Big(1 - \frac{2|k|}{|k| + p}\Big) = -\Big(1 - \frac{2k_{\min}}{k_{\min} + C_p L^{-\beta}}\Big)\\
&= -\Big(1 - \frac{2k_{\min}}{C_p} L^{\beta} + \frac{2k_{\min}^2}{C_p^2} L^{2\beta} - \frac{2k_{\min}^3}{C_p^3} L^{3\beta}\Big) + O(L^{4\beta}),\\
e^{-|k|L} &= 1 - k_{\min} L + \frac{1}{2} k_{\min}^2 L^2 + O(L^3).
\end{aligned}$$

Then the eigenvalue (3.13) can be expanded after a long computation as

$$\lambda_1 = -\Big(1 - \frac{8k_{\min}^3}{abC_p^3} L^{3\beta}\Big) + O(L^{\min\{4\beta,2\}}),$$

which is (3.19). ∎

Now we prove Theorem 3.2.

Proof. Combining Lemma 3.5 and 3.6, the best parameter p is obtained by setting

$$-\lambda_1(k_{\min}, p) = \lambda_1(\bar{k}, p).$$

So by the first equation in (3.17) and (3.19), we see that the optimal parameter should satisfy

$$3\alpha - 3\beta = 1 - \alpha = 3\beta.$$

This implies that $\alpha = \frac{2}{5}$ and $\beta = \frac{1}{5}$. Furthermore, according to the second equation in (3.17), we know that

$$C_k = \Big(3 \cdot \frac{8C_p^3}{a(b-a)}\Big)^{\frac{1}{4}}.$$

Using (3.19) and a direct calculation, the optimal choice of C_p should satisfy the equation

$$\frac{8C_p^3}{abC_k^3} + \Big(1 - \frac{a}{b}\Big)C_k = \frac{8k_{\min}^3}{abC_p^3},$$

which leads to

$$C_p = 2^{-\frac{8}{15}} \Big(\frac{24}{a(b-a)}\Big)^{\frac{1}{5}} k_{\min}^{\frac{4}{5}} = 2^{-\frac{8}{15}} \Big(\frac{12}{1-\sigma^2}\Big)^{\frac{1}{5}} k_{\min}^{\frac{4}{5}}.$$

Substituting this into (3.16), we obtain

$$\lambda_1 = 1 - \frac{16}{ab} \cdot \Big(\frac{a(b-a)k_{\min}}{12}\Big)^{\frac{3}{5}} L^{\frac{3}{5}} + O(L^{\frac{4}{5}}).$$

The corresponding convergence factor (3.11) is then obtained, and this finishes the proof of the overlapping case. Combining with Lemma 3.4, which is the nonoverlapping case, we then have Theorem 3.2. ∎

We compare the convergence factor of the various optimized Schwarz methods to the classical Schwarz methods in Figure 1 on the left. We clearly see that the classical Schwarz method with the $j = 1$ Dirichlet condition converges very badly for low frequencies, the third power in the convergence factor $1-O(L^3)$ which also appears in the abstract Schwarz results in [18, 1, 6, 5] is detrimental for convergence. The new choice of Dirichlet conditions with $j = 3, 4$ for classical Schwarz is already much better. The optimized Schwarz methods have a much further improved low frequency behavior. We also see the local maximum however still appearing, with which equioscillation leads to our new optimized Schwarz methods. On the right, we show the corresponding optimized Schwarz convergence factors without overlap. In Figure 2 we show the corresponding asymptotic convergence factors, more precisely, we plot $1 - \rho$ on the vertical axis, where ρ is the asymptotic convergence factor mentioned above in the paragraph, on the left for the overlapping case when the overlap L becomes small, and

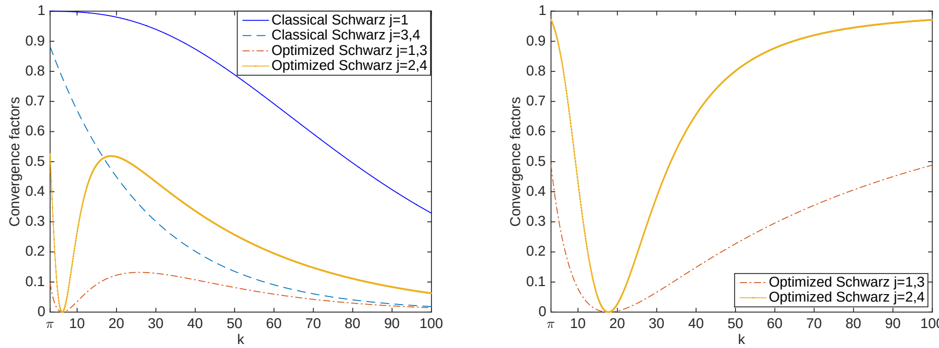

Fig. 1. *Convergence factors with varying k corresponding to an overlap $L = 1/50$ (left) and no overlap (right) for the biharmonic equation and various Schwarz algorithms.*

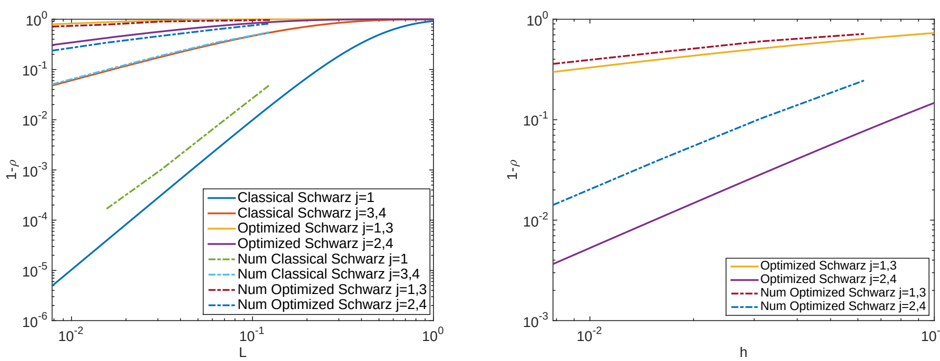

Fig. 2. *Left: convergence factors with varying overlap L and various Schwarz algorithms, and the corresponding numerical results are in dashed. Right: convergence factors with varying meshsize h and various optimized Schwarz algorithms in the nonoverlapping case, and the corresponding numerical results are in dashed.*

on the right without overlap, $L = 0$, when the mesh size h becomes small, meaning that $k_{\max} \sim \frac{1}{h}$ becomes large.

We see that our asymptotic analysis captures very well the best possible performance obtained by numerical optimization and shown in dashed, and the performance of the optimized variants is many orders of magnitude better than for classical Schwarz methods.

3.3. Well-posedness of our choices of parameters. Not all choices of parameters necessarily lead to well-posed subdomain problems, so this needs to be checked for the parameters obtained in Subsection 3.1 and 3.2. We only give the analysis in a bounded domain, which is more useful in practice. We consider the problem (1.1), and assume that $\Omega := (a_1, a_2) \times (b_1, b_2)$ with $a_1 < 0 \leqslant L < a_2$ is a bounded domain in $\mathbb{R}^2$. Then $\Omega_1 := (a_1, L) \times (b_1, b_2)$ and $\Omega_2 := (0, a_2) \times (b_1, b_2)$. The interfaces Γ_1 and Γ_2 are still $x = L$ and $x = 0$. Then we have

Theorem 3.7. *With the choice of parameters in* (3.5), *for all $p > 0$, the subprob-*

lems (3.1) *and* (3.2) *are well-posed.*

Proof. For the parameter matrix $P = \begin{bmatrix} p_{11} & p_{12} \\ p_{21} & p_{22} \end{bmatrix} = P_1^a = P_2^a$ in (3.5), let

$$a(u,v) := \int_{\Omega_i} \sigma \Delta u \Delta v dxdy + \int_{\Omega_i} (1-\sigma)(\partial_{xx}u\partial_{xx}v + \partial_{yy}u\partial_{yy}v + 2\partial_{xy}u\partial_{xy}v)dxdy.$$

Then according to Green's formula, the variational form of (3.1) and (3.2) for OS_1 and OS_2 is

$$\begin{aligned}
\int_{\Omega_i} \Delta^2 u \cdot v dxdy &= a(u,v) + \int_{\partial\Omega_i} (\partial_n \Delta u + (1-\sigma)\partial_\tau(\partial_{n\tau}u)) \cdot v ds - \int_{\partial\Omega_i} (\Delta u - (1-\sigma)\partial_{\tau\tau}u) \cdot \partial_n v ds \\
&= a(u,v) + \int_{\partial\Omega_i} [\partial_n v \quad v] \begin{bmatrix} -(\Delta u - (1-\sigma)\partial_{\tau\tau}u) \\ \partial_n \Delta u + (1-\sigma)\partial_\tau(\partial_{n\tau}u) \end{bmatrix} ds \\
&= a(u,v) + \int_{\Gamma_i} [\partial_n v \quad v] \begin{bmatrix} p_{11} & p_{12} \\ p_{21} & p_{22} \end{bmatrix} \begin{bmatrix} u \\ \partial_n u \end{bmatrix} ds - \int_{\Gamma_i} [\partial_n v \quad v] \begin{bmatrix} g_A \\ g_B \end{bmatrix} ds \\
&= a(u,v) + \int_{\Gamma_i} [\partial_n v \quad v] \begin{bmatrix} p_{12} & p_{11} \\ p_{22} & p_{21} \end{bmatrix} \begin{bmatrix} \partial_n u \\ u \end{bmatrix} ds - \int_{\Gamma_i} [\partial_n v \quad v] \begin{bmatrix} g_A \\ g_B \end{bmatrix} ds \\
&= \int_{\Omega_i} f v dxdy
\end{aligned}$$

for $\forall v \in V$, where V is the space $\{w \mid \sigma\Delta w \in \mathbb{L}^2(\Omega_i), (1-\sigma)\partial_{xx}w \in \mathbb{L}^2(\Omega_i), (1-\sigma)\partial_{yy}w \in \mathbb{L}^2(\Omega_i), (1-\sigma)\partial_{xy}w \in \mathbb{L}^2(\Omega_i), w \in \mathbb{H}^1(\Omega_i), (1-\sigma)\partial_n w|_{\Gamma_i} \in \mathbb{L}^2(\Gamma_i), \partial_n w + pw|_{\Gamma_i} \in \mathbb{L}^2(\Gamma_i), w|_{\partial\Omega_i \cap \partial\Omega} = 0, \partial_n w|_{\partial\Omega_i\cap\partial\Omega} = 0\}$, which depends on the choice of σ and p in $P_1^a = P_2^a$. Let the bilinear form

(3.20)
$$b(u,v) := \int_{\Gamma_i} [\partial_n v \quad v] \begin{bmatrix} p_{12} & p_{11} \\ p_{22} & p_{21} \end{bmatrix} \begin{bmatrix} \partial_n u \\ u \end{bmatrix} ds = \int_{\Gamma_i} [\partial_n v \quad v] \begin{bmatrix} 2p & (1+\sigma)p^2 \\ (1+\sigma)p^2 & 2p^3 \end{bmatrix} \begin{bmatrix} \partial_n u \\ u \end{bmatrix} ds.$$

By a direct analysis, we can check that $\|w\|_{V,\Omega_i} := [a(w,w) + \|w\|^2_{1,\Omega_i} + b(w,w)]^{\frac{1}{2}}$ is a norm of V, where $\|\cdot\|_{1,\Omega_i}$ is the norm of Sobolev space $\mathbb{H}^1(\Omega_i)$. In fact, if $\sigma \neq 1$, V is equivalent to the space $\{w \mid w \in \mathbb{H}^2(\Omega_i), w|_{\partial\Omega_i\cap\partial\Omega} = 0, \partial_n w|_{\partial\Omega_i\cap\partial\Omega} = 0\}$. However, if $\sigma = 1$, things become different. Based on this observation, the following analysis is given suitable for both cases. The variational form can be written as

$$a(u,v) + b(u,v) = \int_{\Gamma_i} [\partial_n v \quad v] \begin{bmatrix} g_A \\ g_B \end{bmatrix} ds + \int_{\Omega_i} f v dxdy.$$

We first prove the continuity of this form, which is natural. For some constant C, note that

$$a(u,v) \leqslant C a(u,u)^{\frac{1}{2}} a(v,v)^{\frac{1}{2}}, \quad b(u,v) \leqslant C b(u,u)^{\frac{1}{2}} b(v,v)^{\frac{1}{2}}.$$

Then

$$a(u,v) + b(u,v) \leqslant C[a(u,u) + b(u,u)]^{\frac{1}{2}} [a(v,v) + b(v,v)]^{\frac{1}{2}} \leqslant C\|u\|_{V,\Omega_i}\|v\|_{V,\Omega_i}$$

finishes the proof of continuity.

For the coercivity, $\forall v \in V$, note that

$$a(v,v) = \sigma\|\Delta v\|_{0,\Omega_i}^2 + (1-\sigma)|v|_{2,\Omega_i}^2,$$

and

$$b(v,v) = 2p\left[\frac{(1+\sigma)}{2}\|\partial_n v + pv\|_{0,\Gamma_i}^2 + \frac{(1-\sigma)}{2}\|\partial_n v\|_{0,\Gamma_i}^2 + \frac{(1-\sigma)}{2}p^2\|v\|_{0,\Gamma_i}^2\right],$$

where $\|\cdot\|_{0,\Omega_i}$, $|\cdot|_{2,\Omega_i}$ and $\|\cdot\|_{0,\Gamma_i}$ are the $\mathbb{L}^2$ norm in Ω_i, second order seminorm of $\mathbb{H}^2(\Omega_i)$ and $\mathbb{L}^2$ norm on Γ_i. Since $v|_{\partial\Omega_i\cap\partial\Omega} = 0$, and $\partial_n v|_{\partial\Omega_i\cap\partial\Omega} = 0$, then we have $\partial_n v + pv|_{\partial\Omega_i\cap\partial\Omega} = 0$. We know that the regularity of the solution to problem

$$-\Delta v = f_v \text{ in } \Omega_i, \quad \partial_n v + pv = 0 \text{ on } \partial\Omega_i\cap\partial\Omega, \quad \partial_n v + pv = g_v \text{ on } \Gamma_i,$$

is

$$\begin{aligned}\|v\|_{1,\Omega_i} &\leqslant C(\|f_v\|_{0,\Omega_i} + \|g_v\|_{-\frac{1}{2},\partial\Omega_i})\\ &\leqslant C(\|f_v\|_{0,\Omega_i} + \|g_v\|_{0,\partial\Omega_i})\\ &\leqslant C(a(v,v)^{\frac{1}{2}} + b(v,v)^{\frac{1}{2}})\\ &\leqslant C(a(v,v)+b(v,v))^{\frac{1}{2}},\end{aligned}$$

which leads to

$$a(v,v) + b(v,v) \geqslant C\|v\|_{V,\Omega_i}^2.$$

For the right hand side, we have

$$\begin{aligned}&\int_{\Gamma_i}[\partial_n v \quad v]\begin{bmatrix} g_A \\ g_B\end{bmatrix} ds + \int_{\Omega_i} f v dxdy\\ &\leqslant C(\|\partial_n v\|_{0,\Gamma_i}\|g_A\|_{0,\Gamma_i} + \|v\|_{0,\Gamma_i}\|g_B\|_{0,\Gamma_i} + \|f\|_{-1,\Omega_i}\|v\|_{1,\Omega_i})\\ &\leqslant C(\|\partial_n v + pv\|_{0,\Gamma_i}\|g_A\|_{0,\Gamma_i} + \|pv\|_{0,\Gamma_i}\|g_A\|_{0,\Gamma_i} + \|v\|_{0,\Gamma_i}\|g_B\|_{0,\Gamma_i} + \|f\|_{-1,\Omega_i}\|v\|_{1,\Omega_i})\\ &\leqslant C(\|g_A\|_{0,\Gamma_i} b(v,v)^{\frac{1}{2}} + \|g_A\|_{0,\Gamma_i}\|v\|_{1,\Omega_i} + \|g_B\|_{0,\Gamma_i}\|v\|_{1,\Omega_i} + \|f\|_{-1,\Omega_i}\|v\|_{1,\Omega_i})\\ &\leqslant C(\|g_A\|_{0,\Gamma_i}\|v\|_{V,\Omega_i} + \|g_A\|_{0,\Gamma_i}\|v\|_{V,\Omega_i} + \|g_B\|_{0,\Gamma_i}\|v\|_{V,\Omega_i} + \|f\|_{-1,\Omega_i}\|v\|_{V,\Omega_i})\\ &\leqslant C(\|g_A\|_{0,\Gamma_i} + \|g_B\|_{0,\Gamma_i} + \|f\|_{-1,\Omega_i})\|v\|_{V,\Omega_i}.\end{aligned}$$

So we have proved the case OS_1 and OS_2 by Lax-Milgram theorem.

For the case OS_3, by direct computation, we obtain

$$\begin{aligned}(\mathcal{N}_3 + P_3^a\mathcal{D}_3)(u) &= \begin{bmatrix}\partial_n u \\ -\partial_n\Delta u\end{bmatrix} + \begin{bmatrix} p & \frac{1}{2p} \\ 0 & -p\end{bmatrix}\begin{bmatrix} u \\ \Delta u\end{bmatrix}\\ &= \begin{bmatrix}\frac{1}{2p} & 0 \\ -p & 1\end{bmatrix}\left(\begin{bmatrix}\Delta u \\ -\partial_n\Delta u\end{bmatrix} + \begin{bmatrix}2p^2 & 2p \\ 2p^3 & 2p^2\end{bmatrix}\begin{bmatrix} u \\ \partial_n u\end{bmatrix}\right) = \begin{bmatrix}\frac{1}{2p} & 0 \\ -p & 1\end{bmatrix}(\mathcal{N}_1 + P_1^a\mathcal{D}_1)(u),\end{aligned}$$

which leads to the fact that OS_1 and OS_3 are equivalent since $\begin{bmatrix}\frac{1}{2p} & 0 \\ -p & 1\end{bmatrix}$ is invertible for $p > 0$. Following the same approach, we have for the case OS_4

$$(\mathcal{N}_4 + P_4^a\mathcal{D}_4)(u) = \begin{bmatrix}\frac{1}{2p} & 0 \\ -\frac{1}{2}(1+\sigma)p & 1\end{bmatrix}[(\mathcal{N}_2 + P_2^a\mathcal{D}_2)(u)].$$

□

Remark 3.8. According to the proof of Theorem 3.7, we obtain that with the choice of parameters (3.5), the methods OS_1 and OS_3 are equivalent, and OS_2 and OS_4 are also equivalent.

3.4. A general optimized parameter for the nonoverlapping OS_1. The structure of the transmission matrices P_j in (3.5) we optimized comes from the structurally consistent choice indicated by the optimal transmission matrices in (3.3) and (3.4). To check if this choice is indeed a good one, we consider general optimization parameters in OS_1 for the nonoverlapping case $L = 0$. So assume that $P_1^g = \begin{bmatrix} p_{11} & p_{12} \\ p_{21} & p_{22} \end{bmatrix}$, where p_{ij}, $i, j = 1, 2$ are constants that do not depend on each other. Then by a direct calculation, we still have $T_2A_2^{-1} = T_1A_1^{-1}$. Defining

$$d_1 := 2p_{12}|k|^3 - 2p_{21}|k|,\ d_2 := 2p_{12}|k|^3 + 2p_{21}|k|,\ d_3 := 2(p_{11}+p_{22})|k|^2 + p_{12}p_{21} - p_{11}p_{22},\ d_4 := 16p_{12}p_{21}|k|^4,$$

by direct calculation, the two eigenvalues of the matrix $T_1A_1^{-1}$ and $T_2A_2^{-1}$ are

$$\lambda_1 := -\frac{d_1 + \sqrt{d_3^2 - d_4}}{d_2 + d_3}, \quad \lambda_2 := -\frac{d_1 - \sqrt{d_3^2 - d_4}}{d_2 + d_3}. \tag{3.21}$$

Then the contraction factor is

$$\rho(p_{11}, p_{12}, p_{21}, p_{22}) = \max_{|k|_{\min} \leqslant |k| \leqslant |k|_{\max}} \max\{|\lambda_1|^2, |\lambda_2|^2\}. \tag{3.22}$$

To determine the values of each element of P_1^g, we use some restrictions based on the following observations:

1. If $p_{12}p_{21} = 0$, then we have $d_1 = \pm d_2$ and $d_4 = 0$. By (3.21), we obtain $|\lambda_1| = 1$ or $|\lambda_2| = 1$, which implies that the method will not converge. So a necessary condition for convergence is

$$p_{12}p_{21} \neq 0. \tag{3.23}$$

2. According to (3.20) and the discussion in the proof of Theorem 3.7, to guarantee well-posedness of the original problem, we need $b(u, u) \geqslant 0$, i.e. the matrix $\begin{bmatrix} p_{12} & p_{11} \\ p_{22} & p_{21} \end{bmatrix}$ needs to be positive semidefinite, which leads to

$$p_{11} = p_{22}, \quad p_{12} \geqslant 0, p_{21} \geqslant 0, \quad p_{12}p_{21} \geqslant p_{11}p_{22}. \tag{3.24}$$

Now we give details of the analysis. Noticing that only d_3 depends on the value of p_{11}, we fix the values of p_{12}, p_{21} to analyze the variation of p_{11}.

LEMMA 3.9. *If $p_{11} = p_{22} \geqslant 0$, then the optimized choice of the parameters must satisfy the relations*

$$p_{12}p_{21} = p_{11}^2, \quad \frac{p_{21}}{p_{12}} = |k|_{\min}|k|_{\max}. \tag{3.25}$$

The corresponding optimized convergence factor then becomes

$$\rho = \left(\frac{\sqrt{|k|_{\max}} - \sqrt{|k|_{\min}}}{\sqrt{|k|_{\max}} + \sqrt{|k|_{\min}}}\right)^2 < 1. \tag{3.26}$$

Proof. Based on the necessary conditions (3.23) and (3.24), we have $p_{12} > 0, p_{21} > 0$, which implies $d_2 > 0, d_4 > 0$, and combining with the condition $p_{11} \geqslant 0$, we have $d_3 \geqslant 0$. To obtain the exact convergence factor (3.22), we need to consider whether

the value $\sqrt{d_3^2 - d_4}$ is real or complex, so our analysis is divided into two cases:
Case 1: $d_3^2 - d_4 \geqslant 0$, which is equivalent to

$$(p_{12}p_{21} - p_{11}^2)[p_{12}p_{21} - (p_{11} - 4|k|^2)^2] \geqslant 0. \tag{3.27}$$

By direct calculations, we have

$$\frac{\partial \lambda_1}{\partial d_3} = -\frac{d_2 d_3 - d_1\sqrt{d_3^2 - d_4} + d_4}{(d_2 + d_3)^2\sqrt{d_3^2 - d_4}} \quad \text{and} \quad \frac{\partial \lambda_2}{\partial d_3} = \frac{d_2 d_3 + d_1\sqrt{d_3^2 - d_4} + d_4}{(d_2 + d_3)^2\sqrt{d_3^2 - d_4}}. \tag{3.28}$$

If $d_1 \geqslant 0$, then from (3.21) we know that $|\lambda_1| \geqslant |\lambda_2|$. Notice that $\lambda_1 \leqslant 0$, and $d_2^2 d_3^2 \geqslant d_1^2 d_3^2$ implies $\frac{\partial \lambda_1}{\partial d_3} < 0$. So in this case, the optimal choice is $d_3^2 = d_4$. On the other hand, if $d_1 < 0$, then $|\lambda_1| < |\lambda_2|$. Notice that $\lambda_2 > 0$, and $d_2^2 d_3^2 \geqslant d_1^2 d_3^2$ implies $\frac{\partial \lambda_2}{\partial d_3} > 0$. So in this case, the optimal choice is also $d_3^2 = d_4$. The condition $d_3^2 = d_4$ means $p_{12}p_{21} - p_{11}^2 = 0$ or $p_{12}p_{21} - (p_{11} - 4|k|^2)^2 = 0$, however, the parameters are required to be constants independent of k, which lead to $p_{12}p_{21} = p_{11}^2$. With these observation, we have

$$|\lambda_1| = |\lambda_2| = \left|\frac{d_1}{d_2 + \sqrt{d_4}}\right| = \left|\frac{2|k|(p_{12}|k|^2 - p_{21})}{2|k|(p_{12}|k|^2 + p_{21} + 2\sqrt{p_{12}p_{21}}|k|)}\right| = \left|\frac{\sqrt{p_{12}}|k| - \sqrt{p_{21}}}{\sqrt{p_{12}}|k| + \sqrt{p_{21}}}\right|.$$

To obtain the optimal convergence rate, we need $\min\limits_{p_{12},p_{21}} \max\limits_{|k|_{\min} \leqslant |k| \leqslant |k|_{\max}} \left|\frac{\sqrt{p_{12}}|k| - \sqrt{p_{21}}}{\sqrt{p_{12}}|k| + \sqrt{p_{21}}}\right|^2$. The optimal choice of these parameters satisfies

$$\frac{\sqrt{p_{21}}}{\sqrt{p_{12}}} = \sqrt{|k|_{\min}|k|_{\max}},$$

and the corresponding convergence factor is (3.26).
Case 2: $d_3^2 - d_4 \leqslant 0$. Then we have $|\lambda_1|^2 = |\lambda_2|^2 = \frac{d_1^2 + d_4 - d_3^2}{(d_2 + d_3)^2}$. By direct calculations, we have $\frac{\partial(|\lambda_1|^2)}{\partial d_3} = \frac{\partial(|\lambda_2|^2)}{\partial d_3} \leqslant 0$. Similarly, the best choice is $d_3^2 = d_4$ and we have the same result as case 1, $|\lambda_1|^2 = |\lambda_2|^2 = \frac{d_1^2}{(d_2 + d_3)^2}$. ∎

LEMMA 3.10. *If $p_{11} = p_{22} < 0$, then for any p_{12} and p_{21}, the convergence factor*

$$\rho(p_{11}, p_{12}, p_{21}, p_{22}) \geqslant \rho(p_{11}^*, p_{12}^*, p_{21}^*, p_{22}^*), \tag{3.29}$$

where $p_{11}^*, p_{12}^*, p_{21}^*, p_{22}^*$ are the parameters we chose in Lemma 3.9.

Proof. Similar as in Lemma 3.9, we divide the proof into two cases.
Case 1: $d_3^2 - d_4 \geqslant 0$. Then implied by the second and third relation in (3.24), (3.27) and $p_{11} < 0$, we have two different conditions, one is $p_{12}p_{21} - (p_{11} - 4|k|^2)^2 \geqslant 0$, which leads to $d_3 = p_{12}p_{21} - p_{11}^2 + 4p_{11}|k|^2 \geqslant 16|k|^4 - 4p_{11}|k|^2 \geqslant 0$, and the other is $p_{11}^2 = p_{12}p_{21}$.

First we assume $d_3 \geqslant 0$. If $d_1 \geqslant 0$, then from (3.21) we know that $|\lambda_1| \geqslant |\lambda_2|$. Notice that $\lambda_1 \leqslant 0$, and $d_2^2 d_3^2 \geqslant d_1^2 d_3^2$ implies $\frac{\partial \lambda_1}{\partial d_3} < 0$. So in this case, the optimal choice is $d_3^2 = d_4$. On the other hand, if $d_1 < 0$, then $|\lambda_1| < |\lambda_2|$. Notice that $\lambda_2 > 0$, and $d_2^2 d_3^2 \geqslant d_1^2 d_3^2$ implies $\frac{\partial \lambda_2}{\partial d_3} > 0$. So in this case, the optimal choice is also $d_3^2 = d_4$. Then similar as in the proof in Lemma 3.9, we also obtain

$$|\lambda_1| = |\lambda_2| = \left|\frac{d_1}{d_2 + \sqrt{d_4}}\right| = \left|\frac{2|k|(p_{12}|k|^2 - p_{21})}{2|k|(p_{12}|k|^2 + p_{21} + 2\sqrt{p_{12}p_{21}}|k|)}\right| = \left|\frac{\sqrt{p_{12}}|k| - \sqrt{p_{21}}}{\sqrt{p_{12}}|k| + \sqrt{p_{21}}}\right|.$$

Second, we assume $p_{11}^2 = p_{12}p_{21}$, then $d_3^2 = d_4$, but $p_{11} < 0$ leads to $d_3 < 0$, which is different from the proof of Lemma 3.9 and implies

$$|\lambda_1| = |\lambda_2| = \left|\frac{d_1}{d_2 - \sqrt{d_4}}\right| = \left|\frac{2|k|(p_{12}|k|^2 - p_{21})}{2|k|(p_{12}|k|^2 + p_{21} - 2\sqrt{p_{12}p_{21}}|k|)}\right| = \left|\frac{\sqrt{p_{12}}|k| + \sqrt{p_{21}}}{\sqrt{p_{12}}|k| - \sqrt{p_{21}}}\right| \geqslant 1.$$

Case 2: $d_3^2 - d_4 \leqslant 0$. Then we have $|\lambda_1|^2 = |\lambda_2|^2 = \frac{d_1^2+d_4-d_3^2}{(d_2+d_3)^2}$, and $\frac{\partial(|\lambda_1|^2)}{\partial d_3} = \frac{\partial(|\lambda_2|^2)}{\partial d_3} = \frac{-2d_1^2-2d_4-2d_2d_3}{(d_2+d_3)^3}$. We know that by (3.24), the inequality $d_2 + d_3 \geqslant 0$ holds. Since we always have $d_2 > 0$ and $d_4 > 0$, if $d_3 \leqslant 0$, then by a direct calculation $-2d_1^2 - 2d_4 - 2d_2d_3 \leqslant -2(d_1^2 + d_4 - d_2^2) = 0$, i.e. $\frac{\partial(|\lambda_1|^2)}{\partial d_3} = \frac{\partial(|\lambda_2|^2)}{\partial d_3} \leqslant 0$. If $d_3 \geqslant 0$, then $\frac{\partial(|\lambda_1|^2)}{\partial d_3} = \frac{\partial(|\lambda_2|^2)}{\partial d_3} \leqslant 0$. Based on this observation, the best choice satisfies the condition $d_3 = \sqrt{d_4}$, and the corresponding convergence factor is

$$|\lambda_1|^2 = |\lambda_2|^2 = \frac{d_1^2}{(d_2 + \sqrt{d_4})^2} = \left|\frac{\sqrt{p_{12}}|k| - \sqrt{p_{21}}}{\sqrt{p_{12}}|k| + \sqrt{p_{21}}}\right|^2.$$

Therefore, no matter which case, the best choice of the parameters p_{12} and p_{21} is the same as Lemma 3.9, which leads to the same convergence factor. However, since $p_{11} < 0$, according to the above discussion, the best choice of parameters should satisfy $d_3 \geqslant 0$, i.e. condition $d_3 = \sqrt{d_4}$ indicates $p_{12}p_{21} - (p_{11} - 4|k|^2)^2 = 0$, which means the parameter p_{11} depends on k. So the inequality (3.29) holds, and "=" happens only for some particular k. ∎

Combining now Lemma 3.9 and 3.10, we have the following result on the relations that must be satisfied by the optimized parameters.

THEOREM 3.11. *For OS_1 without overlap, if we allow the use of the general matrix*

$$P_1^g = \begin{bmatrix} p_{11} & p_{12} \\ p_{21} & p_{22} \end{bmatrix}, \tag{3.30}$$

then the optimized choice of the parameters must satisfy

$$p_{11} = p_{22} \geq 0, \quad p_{12}p_{21} = p_{11}^2, \quad \frac{p_{21}}{p_{12}} = k_{\min}k_{\max}. \tag{3.31}$$

Remark 3.12. A direct comparison with our structurally consistent choice shows that it does indeed satisfy these conditions, and is thus the good simplifying choice, i.e. P_1^a in (3.6) satisfies all the conditions in (3.31). Further, we also find that $\widetilde{P}_1^a := \mu P_1^a$, where μ is some positive constant, still satisfies the conditions in (3.31) and is another good choice.

Remark 3.13. All our analyses are based on the Fourier transform for the unbounded problem in the two-subdomain case. For the bounded domain case, we can do the analysis in a similar way by Fourier series. For example, if we set the simply supported condition ($\mathcal{D}_4$) on the boundary, the corresponding Fourier modes are $\sin(k\pi y), k \in \mathbb{N}^+$, and then we have the expansion $u(x, y) = \sum_k \widehat{u}(x, k)\sin(k\pi y)$, which leads to a similar form as (2.4). For the extension to the many subdomain case, (2.8) is then changed into $\bar{\mathbf{g}}_1^{n+1} = \prod_i T_i A_i^{-1}\bar{\mathbf{g}}_1^n$. The convergence factor can be obtained by analyzing the eigenvalues of $\prod_i T_i A_i^{-1}$, which is more complicated and left for future work.

TABLE 1
Iteration numbers for the three classical Schwarz methods for different values of the overlap L.

	CS_1				CS_3 and CS_4			
h	$\frac{1}{16}$	$\frac{1}{32}$	$\frac{1}{64}$	$\frac{1}{128}$	$\frac{1}{16}$	$\frac{1}{32}$	$\frac{1}{64}$	$\frac{1}{128}$
$L = h$	685	5167	40265	> 200000	34	68	134	267
$L = 2h$	191	1332	10127	81942	17	35	68	134
$L = 4h$	41	244	1768	13694	9	18	34	67

Remark 3.14. Note that our methods are based on a two-dimensional setting. For the problem in 3D, we can extend our methods naturally: let $n = (n_x, n_y, n_z)$ be the unit normal direction and $\nabla = (\partial_x, \partial_y, \partial_y)$ be the gradient in 3D. Then the conditions $\Delta u - (1-\sigma)\partial_{\tau\tau}u$ and $-\partial_n \Delta u - (1-\sigma)\partial_\tau(\partial_{n\tau}u)$ in 2D case on the boundary become $\Delta u - (1-\sigma)(n \times \nabla) \cdot (n \times \nabla)u$ and $-\partial_n \Delta u - (1-\sigma)(n \times \nabla) \cdot [(n \cdot \nabla) \cdot (n \times \nabla)u]$ in 3D. Fourier analyses then also works for this problem, by transforming two directions rather than one.

Remark 3.15. The idea of this paper can be extended to general $2m$th-order problems. In [16], it is shown that Schwarz methods for $2m$th-order problems

$$(-\Delta)^m u = f$$

with classical Dirichlet boundary conditions $\mathcal{D}(u) = [u \ \partial_n u \ ... \ \partial^{m-1}_{n^{m-1}} u]$ have convergence factors of the form $1 - O(L^{2m-1})$. Naturally, in our opinion, by choosing Dirichlet boundary conditions like $\mathcal{D}(u) = [u \ \Delta u \ ... \ \Delta^{m-1} u]$, the corresponding convergence factor should be $1 - O(L)$, which is as good as the Schwarz method for Laplace's equation. Other boundary conditions and optimized Schwarz methods are left for future work.

4. Numerical results. We study now our algorithms CS_j $j = 1, 3, 4$ and OS_j $j = 1, 2, 3, 4$ for the biharmonic equation (1.1) numerically in the square domain $\Omega = (0, 1) \times (0, 1)$ with Dirichlet boundary condition $\mathcal{D}_1(u) = \mathbf{0}$. We choose for the right hand side $f := 24y^2(1-y)^2 + 24x^2(1-x)^2 + 8[(1-2x)^2 - 2(x-x^2)][(1-2y)^2 - 2(y-y^2)]$, which corresponds to the manufactured solution $u = x^2(1-x)^2y^2(1-y)^2$. We discretize (1.1) using the classical 13-point finite difference scheme, see, e.g., [9]. We first use two subdomains Ω_1 and Ω_2, and stop the Schwarz iterations when $\max_i \frac{\|u_i^n - u\|_{l^2}}{\|u\|_{l^2}} \leqslant 10^{-6}$, where u_i^n is the discrete subdomain iterate on Ω_i at step n, and u is the discrete mono-domain solution obtained by a direct solver. We start the iteration with a random initial guess which is important, since if we choose some special initial guess, the methods may converge faster than in the worst case covered by our analysis, which then does not reveal the real convergence rate, see [8, Figure 5.2].

We start with two equal subdomains, the interface being in the middle, and show in Table 1 the iteration numbers the three classical Schwarz algorithms CS_j, $j = 1, 3, 4$ require to solve the problem, depending on the mesh size h with $L = O(h)$. We see that all three classical Schwarz algorithms deteriorate when the mesh is refined, but CS_3 and CS_4 convergence much faster than the truly classical CS_1 for the biharmonic problem, which illustrates well Theorem 2.1 and Theorem 2.2. We show in Table 2, the corresponding results for the optimized Schwarz methods OS_j, $j = 1, 2, 3, 4$, where the optimized parameters for OS_1, OS_3 and OS_2, OS_4 are chosen according to Theorem 3.1 and 3.2. Because the size of the domain in the y direction is 1, we know that the

TABLE 2
Iteration numbers for the four optimized Schwarz methods for different values of the overlap L.

	OS_1 and OS_3				OS_2 and OS_4			
h	$\frac{1}{16}$	$\frac{1}{32}$	$\frac{1}{64}$	$\frac{1}{128}$	$\frac{1}{16}$	$\frac{1}{32}$	$\frac{1}{64}$	$\frac{1}{128}$
$L=h$	6	7	10	12	15	23	34	52
$L=2h$	4	6	7	10	9	15	23	34
$L=4h$	4	4	6	7	6	9	15	23

TABLE 3
Iteration numbers for the four optimized Schwarz methods for different values of the overlap L with the Golden Gate Bridge example.

	OS_1 and OS_3				OS_2 and OS_4			
L	$L=0$	$L=h$	$L=2h$	$L=4h$	$L=0$	$L=h$	$L=2h$	$L=4h$
iter	46	12	9	7	4167	48	32	21

smallest wavelength captured by this domain size is $\lambda = 2$, then we set $k_{\min} = \frac{2\pi}{\lambda} = \pi$ here. We see that convergence is drastically improved, and the iteration numbers are now only weakly depending on the overlap and mesh size, as predicted by our analysis.

We finally show experiments which go beyond our detailed two subdomain analysis, namely a numerical simulation for the Golden Gate Bridge with many subdomains, which was also used to test Dirichlet-Neumann methods in [11]. We only show the optimized Schwarz methods here, because the performances are superior to the classical Schwarz methods with much lower iteration numbers according to the two subdomains case. The famous Golden Gate Bridge is a suspension bridge with two towers and total length of 2737 meters, and the span between the two towers to simulate is about 1280 meters. With the body supported by the towers and the suspension cables, i.e. the boundary conditions $\mathcal{D}_4$, the problem is

$$\Delta^2 u = f \quad \text{in } \Omega, \quad \mathcal{D}_4(u) = 0 \quad \text{on } \partial\Omega.$$

The bridge is only 27.4 meters wide, and with $\Omega = (0, 1280) \times (0, 27.4)$, a decomposition into 50 bridge segments forming the subdomains Ω_i of size 25.6×27.4 is natural. Since the bridge construction is steel, we set $\sigma = 0.28$ for the outside boundary. We also set the optimized parameters for OS_1, OS_3 and OS_2, OS_4 according to Theorem 3.1 and 3.2, where $\sigma = 1$ for OS_1 and OS_3 and $\sigma = 0$ for OS_2 and OS_4 on the interface for the iteration. As source, we use randomly placed cars, trucks, and vans on the bridge section we simulate, see the top in Figure 3. The displacement of the bridge under this load is the solution of our biharmonic problem, shown at the bottom of Figure 3. We see that the bridge is very stable under this load, the displacement is very small. We also use $\max_i \frac{\|u_i^n - u\|_{l^2}}{\|u\|_{l^2}} \leqslant 10^{-6}$ as the iteration termination condition here. The iteration numbers for our optimized Schwarz methods are shown in Table 3. This shows that also in this many subdomain case beyond our analysis, the optimized Schwarz methods OS_1 and OS_3 are much better algorithms than OS_2 and OS_4 for solving the biharmonic problem.

5. Conclusions. As was shown in [11], there are many choices of Dirichlet and Neumann conditions for biharmonic problems, and one obtains thus various Dirichlet-Neumann domain decomposition algorithms with different convergence rates. Here, we first studied the classical Schwarz method by choosing different Dirichlet condi-

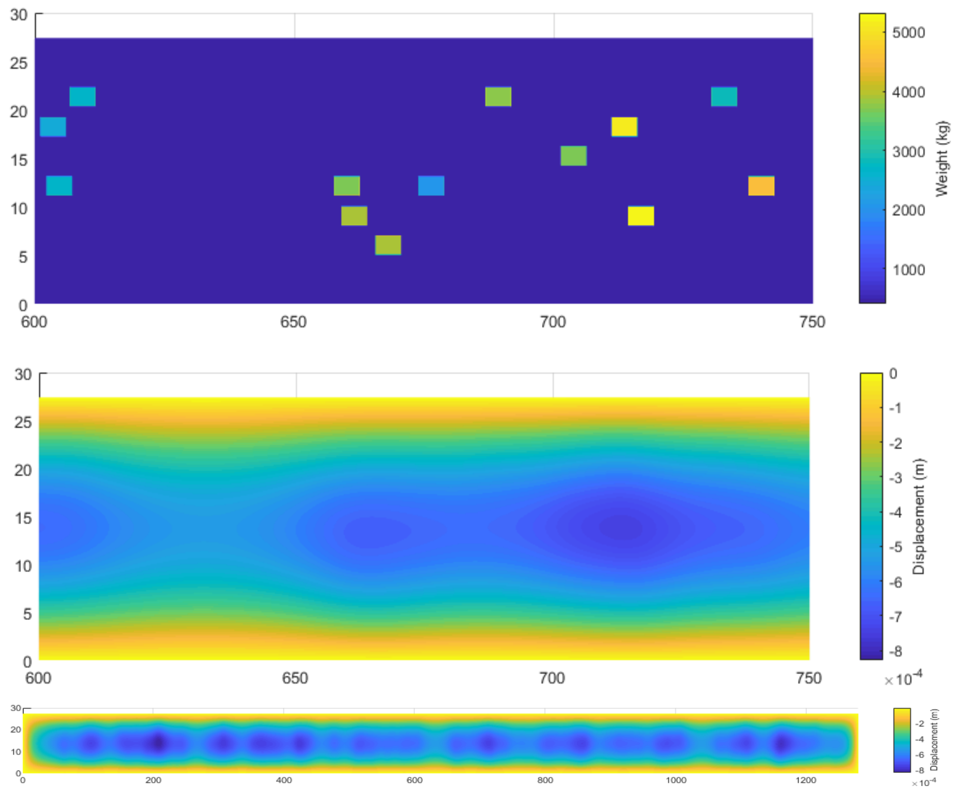

FIG. 3. *Top: the six-lane bridge section* $[600, 750]$ *with different car, truck and van weights randomly placed. Middle: displacement of the bridge caused by this load in the same bridge section* $[600, 750]$. *Bottom: Displacement caused by this load of the entire bridge, scaled by 4 for better visibility.*

tions, and we showed that the convergence rate for two of them is much better than the classical choice, namely like for the Laplace problem. We then proposed new optimized Schwarz methods by linearly combining different Dirichlet and Neumann conditions. Our analysis of the convergence rates shows that they all converge substantially better than the classical Schwarz method, even when it is using the Dirichlet condition leading to similar performance as Schwarz methods applied to Laplace problems.

REFERENCES

[1] S. C. BRENNER, *A two-level additive Schwarz preconditioner for nonconforming plate elements*, Numerische Mathematik, 72 (1996), pp. 419–447.

[2] C. R. DOHRMANN, *A preconditioner for substructuring based on constrained energy minimization*, SIAM Journal on Scientific Computing, 25 (2003), pp. 246–258.

[3] V. DOLEAN, F. NATAF, AND G. RAPIN, *How to use the Smith factorization for domain decomposition methods applied to the Stokes equations*, in Domain decomposition methods in science and engineering XVII, Springer, 2008, pp. 477–484.

[4] C. FARHAT AND J. MANDEL, *The two-level FETI method for static and dynamic plate problems Part I: An optimal iterative solver for biharmonic systems*, Computer methods in applied mechanics and engineering, 155 (1998), pp. 129–151.

[5] X. FENG AND O. A. KARAKASHIAN, *Two-level non-overlapping Schwarz preconditioners for*

a discontinuous Galerkin approximation of the biharmonic equation, Journal of Scientific Computing, 22 (2005), pp. 289–314.

[6] X. Feng and T. Rahman, *An additive average Schwarz method for the plate bending problem*, (2002).

[7] M. J. Gander, *Optimized Schwarz methods*, SIAM Journal on Numerical Analysis, 44 (2006), pp. 699–731.

[8] M. J. Gander, *Schwarz methods over the course of time*, Electronic transactions on numerical analysis, 31 (2008), pp. 228–255.

[9] M. J. Gander and F. Kwok, *Chladni figures and the Tacoma bridge: motivating PDE eigenvalue problems via vibrating plates*, SIAM Review, 54 (2012), pp. 573–596.

[10] M. J. Gander and Y. Liu, *On the definition of Dirichlet and Neumann conditions for the biharmonic equation and its impact on associated Schwarz methods*, in Domain Decomposition Methods in Science and Engineering XXIII, Springer, 2017, pp. 303–311.

[11] M. J. Gander and Y. Liu, *Is there more than one Dirichlet–Neumann algorithm for the biharmonic problem?*, SIAM Journal on Scientific Computing, 43 (2021), pp. A1881–A1906.

[12] P. Gervasio, *Homogeneous and heterogeneous domain decomposition methods for plate bending problems*, Computer methods in applied mechanics and engineering, 194 (2005), pp. 4321–4343.

[13] P. Le Tallec, J. Mandel, and M. Vidrascu, *A Neumann–Neumann domain decomposition algorithm for solving plate and shell problems*, SIAM Journal on Numerical Analysis, 35 (1998), pp. 836–867.

[14] J. Mandel and C. R. Dohrmann, *Convergence of a balancing domain decomposition by constraints and energy minimization*, Numerical linear algebra with applications, 10 (2003), pp. 639–659.

[15] J. Mandel, R. Tezaur, and C. Farhat, *A scalable substructuring method by Lagrange multipliers for plate bending problems*, SIAM Journal on Numerical Analysis, 36 (1999), pp. 1370–1391.

[16] J. Park, *Two-level overlapping Schwarz preconditioners with universal coarse spaces for* $2m$ *th-order elliptic problems*, 2024, https://arxiv.org/abs/2403.18970.

[17] Y.-q. Shang and Y.-n. He, *Fourier analysis of Schwarz domain decomposition methods for the biharmonic equation*, Applied Mathematics and Mechanics, 30 (2009), pp. 1177–1182.

[18] X. Zhang, *Two-level Schwarz methods for the biharmonic problem discretized conforming c^1 elements*, SIAM journal on numerical analysis, 33 (1996), pp. 555–570.